Stability of spectral collocation schemes with explicit-implicit-null time-marching for convection-diffusion and convection-dispersion equations

Meiqi Tan[1], Juan Cheng[2], and Chi-Wang Shu[3]

Abstract

In this paper, we discuss the Fourier collocation and Chebyshev collocation schemes coupled with two specific high order explicit-implicit-null (EIN) time-marching methods for solving the convection-diffusion and convection-dispersion equations. The basic idea of the EIN method discussed in this paper is to add and subtract an appropriate large linear highest derivative term on one side of the considered equation, and then apply the implicit-explicit time-marching method to the equivalent equation. The EIN method so designed does not need any nonlinear iterative solver, and the severe time step restriction for explicit methods can be removed. We give stability analysis for the proposed EIN Fourier collocation schemes on simplified linear equations by the aid of the Fourier method. We show rigorously that the resulting schemes are stable with particular emphasis on the use of large time steps if appropriate stabilization parameters are chosen. Even though the analysis is only performed on the EIN Fourier collocation schemes, numerical results show that the stability criteria can also be extended to the EIN Chebyshev collocation schemes. Numerical experiments are given to demonstrate the stability, accuracy and performance of the EIN schemes for both one-dimensional and two-dimensional linear and nonlinear equations.

Keywords: Convection-diffusion equation, convection-dispersion equation, stability, explicit-implicit-null time discretization, Fourier collocation method, Chebyshev collocation method, Fourier analysis.

[1]Graduate School, China Academy of Engineering Physics, Beijing 100088, China. E-mail: tanmeiqi20@gscaep.ac.cn.

[2]Corresponding author. Laboratory of Computational Physics, Institute of Applied Physics and Computational Mathematics, Beijing 100088, China and HEDPS, Center for Applied Physics and Technology, and College of Engineering, Peking University, Beijing 100871, China. E-mail: cheng_juan@iapcm.ac.cn. Research is supported in part by NSFC grants 12031001 and 11871111, and CAEP Foundation No. CX20200026.

[3]Division of Applied Mathematics, Brown University, Providence, RI 02912. E-mail: chi-wang_shu@brown.edu. Research is supported in part by NSF grant DMS-2010107 and AFOSR grant FA9550-20-1-0055.

1 Introduction

In this paper, we will discuss the Fourier collocation and Chebyshev collocation methods coupled with two different explicit-implicit-null (EIN) time-marching methods for the convection-diffusion and convection-dispersion equations, respectively, with an eye to basic questions of accuracy and stability of the schemes. We restrict the description to problems in one dimension for symbolic simplicity, although the conclusions are verified to hold also for two-dimensional equations in the numerical experiment sections.

The convection-diffusion equation

$$U_t + f(U)_x - \mathcal{D}(U)_{xx} = 0, \qquad \mathcal{D}(U) = \int^U d(s)ds, \tag{1.1}$$

where $d(s) \geq 0$ is smooth and bounded, has been used in many areas of science and technology; e.g., fluid dynamics, heat transfer and environmental protection. For an extensive literature devoted to the above equation let us mention the papers [20, 39], and the references therein. Here and below, we use the capital letter U to denote the exact solution of the considered equation.

The convection-dispersion equation

$$U_t + f(U)_x + \mathcal{G}(U_x)_{xx} = 0 \tag{1.2}$$

is a special KdV-type equation typified by the Korteweg-de Vries (KdV) equation [26] and its generalizations. The KdV-type equations, whose travelling-wave solutions called solitary waves play an important role in the long-term evolution of initial data [5], have especially important applications as a widely used model of nonlinear dispersion in fluid dynamics and plasma physics.

For the above two equations, the Fourier collocation method is a popular numerical method, which grants the use of the fast Fourier transform. However, a disadvantage of the use of the Fourier basis is the confinement to periodic boundary condition. In some situations, one may want to consider the problems involving non-periodic boundary conditions. In this

case, we can turn to the pseudo-spectral Chebyshev method, i.e., a collocation method at the Chebyshev Gauss nodes. There is an extensive body of bibliography [1,6,7,12,22,33] on the numerical simulation and analysis of the convection-diffusion and convection-dispersion equations in conjunction with the Fourier collocation or Chebyshev collocation method for spatial discretization. We refer to [1, 12, 33] for the convection-dispersion equation, and to [6, 7, 22] for the convection-diffusion equation. Limited by the time-marching method, to our knowledge, no high order numerical schemes can efficiently simulate the above two kinds of time-dependent equations with nonlinear highest derivative terms at large time steps whilst keeping stability, especially when the Chebyshev collocation method is used for spatial discretization.

Time discretization is a very important issue for time-dependent partial differential equations (PDE). The explicit time-marching methods are easy to implement, however, they become unfeasible with growing spatial order due to the worsening stiffness of the high order derivative terms. For example, for the convection-dispersion equation with the Chebyshev collocation method for spatial discretization, the explicit method may suffer from $\tau = O(N^{-6})$ for stability, where τ is the time step and N is the number of the Chebyshev collocation points. Stable implicit methods exist for virtually any order and they are usually free of time step restriction [23]. However, they are cumbersome for nonlinear equations, since a nonlinear algebraic system must be solved at each time step. Usually, the nonlinear system can be linearized by the Newton-type method or by construction, as in the case of Rosenbrock-type Runge-Kutta methods [4]. However, the resulting linear system requires a great deal of computation and storage of the exact or approximate Jacobian of the nonlinear operator, which are typically non-symmetric and often ill-conditioned. In addition, the fast solution of the system usually depends on an efficient preconditioner, which may be hard to get. These difficulties diminish the benefits of implicit methods considerably. The implicit-explicit (IMEX) methods [2,3,8,9], which treat the stiffer terms implicitly and the rest of the terms explicitly, can not only alleviate time step restriction, but also reduce the difficulty

of solving the algebraic equations especially when the high order derivative terms of the equation are linear. However, for the equations with nonlinear highest derivative terms, the method is still too expensive to use. To resolve this issue, the explicit-implicit-null method has been proposed and analyzed.

Here we give a brief introduction to the EIN method considered in this paper. The basic idea of the method is to add and subtract an appropriately large linear term, which needs to have the same scale in wavenumber as the most stiff term, on one side of the equation and then apply the IMEX method to the equivalent equation. In a recent study, Duchemin and Eggers [17] proposed to call this procedure the "explicit-implicit-null method", or EIN method for short, since the piece added to the equation is then subtracted, seemingly adding zero. In this paper, an equal highest derivative term with constant coefficient is added to and subtracted from one side of the equation. Taking the convection-diffusion equation (1.2) as an example, we add and subtract a term with constant diffusion coefficient $a_1 U_{xx}$ at the left-hand side of the considered PDE

$$U_t + \underbrace{f(U)_x + a_1 U_{xx} - \mathcal{D}(U)_{xx}}_{T_1} - \underbrace{a_1 U_{xx}}_{T_2} = 0, \qquad a_1 = a_0 \times \max_U d(U), \tag{1.3}$$

where $\mathcal{D}(U) = \int^U d(s)ds$ and $d(U) \geq 0$ is smooth and bounded, and then treat T_1 and T_2 separately. Here, $a_0 > 0$ is a constant yet to be determined. The hope is that the damping term T_2 is large enough to suppress the unstable high wavenumber modes in T_1 such that T_1 is either not stiff, or less stiff and less dissipative compared to T_2, thus it can be treated explicitly, and T_2 is stiff and dissipative, thus will be discretized implicitly. The explicit treatment of T_1 and the implicit discretization of the linear term T_2 lead to a linear system, which is relatively easy to solve by many iterative methods. This offers an enormous advantage over the pure IMEX method.

The EIN method has been implemented previously by a number of authors on a case-by-case basis. As far as we could tell, the EIN method was first proposed and adopted by Douglas and Dupont [16] to assure the stability for nonlinear diffusion equations in conjunction with

an alternating direction Galerkin method for spatial discretization. Subsequently, it was used to stabilize the viscous free-surface dynamics of two liquid drops during coalescence [18], and the coarsening kinetics of interconnected two-phase mixtures [43]. In addition, the method has also been applied with success to, for example, the level set equations for mean curvature flow and motion by surface diffusion [37], the continuum models for the evolution of the molecular beam epitaxy growth [42], the Boltzmann kinetic equations and related problems with nonlinear stiff sources [21], the Cahn-Hilliard equations [36], the diffusion equations [40] with the local discontinuous Galerkin (LDG) method for spatial discretization, etc. These papers provide a clean description on the size of the constant a_0, which is closely related to the equations discussed, the IMEX time-marching methods adopted and the auxiliary term added to and subtracted from the equation. However, the discussion of the method in these papers is limited to the first and second order in time. In a recent work [38], the third order EIN schemes coupled with the finite difference and LDG methods for the high order dissipative and dispersive equations were considered. However, stability analysis was just performed on the linear equations with the highest derivative terms. The EIN method is similar to the stabilization method [13,14,24,27–29] in the stabilization mechanism. Roughly speaking, for a p-th order scheme, the basic idea of the the stabilization method is to add an additional $O(\tau^p)$ well-chosen stabilizing term of the form

$$a_1 \tau^{p-1} B(u^{n+1} - u^n) \tag{1.4}$$

to the numerical scheme, where B is a general operator and u^n is the numerical solution at the n-th time level. One example is $B = \partial_{xx}$ for the convection-diffusion equation. The $O(\tau^p)$ term vanishes as $\tau \to 0$ and the numerical solution is expected to converge to the true PDE solution. When a simple low order IMEX time-marching method is adopted, the EIN method sometimes can also be viewed as the stabilization method since the stabilizing term generated by the implicit and explicit time-marching of the auxiliary term added to and subtracted from the equation is consistent with (1.4). However, this is not the case for the high order IMEX time-marching methods, because the stabilizing term introduced by the

EIN method is much more complex than the one introduced by the stabilization method.

Although the EIN methods have been developed in many literatures, to the best of our knowledge, there are very few applications and analyses of the EIN methods for the convection-diffusion and convection-dispersion equations in conjunction with the Fourier collocation or Chebyshev collocation method for spatial discretization, especially with the Chebyshev collocation method. In this paper we discuss the Fourier collocation and Chebyshev collocation schemes coupled with two carefully tailored EIN time discretizations for the convection-diffusion and convection-dispersion equations, respectively. One is a second order EIN multi-step method (EIN-MS2), the other is a third order EIN Runge-Kutta method (EIN-RK3). We provide stability analysis for the EIN schemes with pseudo-spectral Fourier spatial discretization by the aid of the Fourier method. Our main contribution is to show rigorously that the resulting EIN Fourier collocation schemes are stable with particular emphasis on the use of large time steps if appropriate stabilization parameters a_0 are chosen. Even though the analysis is only performed on the simplified linear equations, numerical experiments show that the proposed schemes are stable and can achieve optimal orders of accuracy for both one-dimensional and two-dimensional linear and nonlinear equations. In addition, the EIN schemes with pseudo-spectral Chebyshev spatial discretization are shown to be stable as long as the values of a_0 are consistent with those of the EIN Fourier collocation schemes. In Table 1.1, we summarize the stability conditions of the EIN schemes with the Fourier collocation and Chebyshev collocation methods for the convection-diffusion and convection-dispersion equations, where τ_0 is a constant, C is the Courant number and N is the number of the collocation points. Notice that the specific choices of the temporal and spatial discretizations may change the values of C and τ_0, but not the generic types of the time step constraints listed in this table.

Our work is organized in the following way. In Section 2, we present the spatial discretizations and the time-marching methods for the convection-diffusion equation. The standard Fourier techniques are used to analyze the stability of the schemes in the linear case. In

Table 1.1: The stability conditions of the EIN schemes with the Fourier collocation and Chebyshev collocation methods for the convection-diffusion and convection-dispersion equations.

equation	convection-diffusion		convection-dispersion	
method	Fourier collocation	Chebyshev collocation	Fourier collocation	Chebyshev collocation
EIN-MS2	$a_1 > 0.5 \max_U d(U)$ $\tau \le CN^{-1}$	$a_1 > 0.5 \max_U d(U)$ $\tau \le CN^{-2}$	$a_1 > 0.5 \max_{U_x} \lvert\mathcal{G}'(U_x)\rvert$ $\tau \le \max\{CN^{-1}, \tau_0\}$	$a_1 > 0.5 \max_{U_x} \lvert\mathcal{G}'(U_x)\rvert$ $\tau \le CN^{-2}$
EIN-RK3	$a_1 \ge 0.54 \max_U d(U)$ $\tau \le \max\{CN^{-1}, \tau_0\}$	$a_1 \ge 0.54 \max_U d(U)$ $\tau \le CN^{-2}$	$a_1 \ge 0.54 \max_{U_x} \lvert\mathcal{G}'(U_x)\rvert$ $\tau \le \max\{CN^{-1}, \tau_0\}$	$a_1 \ge 0.54 \max_{U_x} \lvert\mathcal{G}'(U_x)\rvert$ $\tau \le CN^{-2}$

Section 3, we provide a series of numerical tests to examine the stability and performance of the proposed schemes for both one-dimensional and two-dimensional linear and nonlinear problems. Section 4 is similar to Section 2, and Section 5 is similar to Section 3, but they are for the convection-dispersion equations. Finally, the concluding remarks are presented in Section 6.

2 Convection-diffusion equations

In this section, we present the Fourier collocation method, the Chebyshev collocation method and the time-marching methods for the convection-diffusion equation. The standard Fourier techniques are used to analyze the stability of the schemes in the linear case.

2.1 The spatial discretizations

2.1.1 The Fourier collocation method

In this subsection, we use the Fourier collocation method to numerically solve the convection-diffusion equation (1.3) subject to periodic boundary condition and the initial condition

$$U(x,0) = U_0(x), \qquad x \in \Omega. \tag{2.1}$$

Now we recall some basic results about the Fourier collocation method which will be used throughout the paper. For ease of presentation, the spatial period Ω is normalized to $[0, 2\pi]$. For any integer $N > 0$, denote $S_N = \text{span}\{e^{ikx}, -N \le k \le N-1\}$, where $i^2 = -1$. Consider the set of points

$$x_j = \frac{\pi j}{N}, \qquad j = 0, 1, ..., 2N-1, \tag{2.2}$$

referred to as Fourier collocation nodes. The discrete Fourier coefficients of a function u in $[0, 2\pi]$ with respect to these points are

$$\tilde{u}_k = \frac{1}{2N} \sum_{j=0}^{2N-1} u(x_j) e^{-ikx_j}, \qquad -N \le k \le N-1. \tag{2.3}$$

Due to the orthogonality relation

$$\frac{1}{2N} \sum_{j=0}^{2N-1} e^{i\ell x_j} = \begin{cases} 1, & \ell = 2Nm, \quad m = 0, \pm 1, \pm 2, ... \\ 0, & \text{otherwise} \end{cases}, \tag{2.4}$$

we have the inversion formula

$$u(x_j) = \sum_{k=-N}^{N-1} \tilde{u}_k e^{ikx_j}, \qquad j = 0, 1, ..., 2N-1.$$

For a function $u(x) \in C^0(0, 2\pi)$, we define a trigonometric interpolation operator I_N at the Fourier collocation nodes

$$I_N u(x_j) = u(x_j), \qquad j = 0, 1, ..., 2N-1.$$

From (2.4), we have

$$I_N u(x) = \sum_{k=-N}^{N-1} \tilde{u}_k e^{ikx}.$$

The semi-discrete Fourier collocation approximation for the above periodic initial value problem can be defined as follows: find $u_N(t) \in S_N$, such that for all $j = 0, 1, ..., 2N-1$, we have

$$u_N(x, 0) = I_N U_0,$$

$$\Big\{ (u_N)_t + \underbrace{[I_N f(u_N)]_x - [I_N \mathcal{D}(u_N)]_{xx} + a_1 (u_N)_{xx}}_{T_1} \Big\}(x_j, t) = \underbrace{a_1 (u_N)_{xx}}_{T_2}(x_j, t),$$

where $\mathcal{D}(u_N) = \int^{u_N} d(s) ds$, $a_1 = a_0 \times \max_{u_N} d(u_N)$, a_0 is a constant to be determined.

2.1.2 The Chebyshev collocation method

After a suitable mapping normalization, we can assume that the problem is set in the reference space interval $[-1, 1]$. In this subsection, we use the Chebyshev collocation method to numerically solve the convection-diffusion equation (1.3) with the initial condition (2.1) and the Dirichlet-Dirichlet boundary conditions

$$U(-1, t) = g_1(t), \qquad U(1, t) = g_2(t), \qquad 0 \le t \le T, \tag{2.5}$$

where T is the final computing time. For other type boundary conditions we refer the readers to [10, 11, 31] and the references therein.

Now we summarize the notations regarding the Chebyshev collocation method used in this paper. For an overview of the method the readers are referred to [11]. For any integer $N > 0$, let P_N be the space of algebraic polynomials of degree less than or equal to N in $[-1, 1]$. We denote by

$$\tilde{x}_j = -\cos\left(\frac{\pi j}{N}\right), \qquad j = 0, ..., N, \tag{2.6}$$

the nodes of the Gauss-Lobatto integration formula relative to the Chebyshev weight $w(x) = (1 - x^2)^{-1/2}$, $-1 < x < 1$. The Chebyshev collocation approximation for the convection-diffusion equation (1.3) augmented with the initial condition (2.1) and the Dirichlet-Dirichlet boundary conditions (2.5) can be defined as follows: seek for a solution $\bar{u}_N(x, t) \in P_N$ such that for $\tilde{x}_j$, $j = 1, 2, ..., N - 1$ we have

$$\Big\{(\bar{u}_N)_t + \underbrace{[\tilde{I}_N f(\bar{u}_N)]_x - [\tilde{I}_N \mathcal{D}(\bar{u}_N)]_{xx} + a_1(\bar{u}_N)_{xx}}_{T_1}\Big\}(\tilde{x}_j, t) - \underbrace{a_1(\bar{u}_N)_{xx}}_{T_2}(\tilde{x}_j, t) = 0$$

and

$$\bar{u}_N(x, 0) = \tilde{I}_N U_0(x),$$

$$\bar{u}_N(\tilde{x}_0, t) = g_1(t), \qquad \bar{u}_N(\tilde{x}_N, t) = g_2(t),$$

where $\mathcal{D}(\bar{u}_N) = \int^{\bar{u}_N} d(s)ds$, $a_1 = a_0 \times \max_{\bar{u}_N} d(\bar{u}_N)$, a_0 is a constant to be determined and $\tilde{I}_N$ is an interpolation operator defined at the points (2.6).

2.2 The temporal discretizations

Let $\{t^n = n\tau \in [0,T]\}_{n=0}^{M}$ be the time at the n-th time step, in which τ is the time step and T is the final computing time. To give a brief introduction of the time-marching method discussed in this paper, let us consider the following system of ordinary differential equations

$$\frac{\mathrm{d}u}{\mathrm{d}t} = \mathcal{L}(t,u) + \mathcal{N}(t,u),$$

where $\mathcal{L}(t,u)$ is derived from the T_2 term and is treated implicitly, and $\mathcal{N}(t,u)$ arises from the spatial discretization of the T_1 term and is dealt with an explicit way. Given u^n, we would like to find the numerical solution at the next time level t^{n+1}. A second order IMEX multi-step method and a third order IMEX Runge-Kutta method will be considered in this paper. We have also considered other IMEX methods, but we will not state them here to save space.

2.2.1 The second order IMEX multi-step method

Because no multi-step methods of order greater than two can be A-stable, the high order multi-step methods might not be a good choice for matching very high order spatial discretizations and for the high order equations. Therefore, we just consider the second order Crank-Nicolson/Leap-Frog (CN/LF) method

$$\frac{u^{n+1} - u^{n-1}}{2\tau} = \mathcal{N}(t^n, u^n) + \frac{\mathcal{L}(t^{n-1}, u^{n-1}) + \mathcal{L}(t^{n+1}, u^{n+1})}{2}, \tag{2.7}$$

which is preferred in applications. This scheme uses the Leap-Frog method for the explicit part and a Crank-Nicolson type method for the implicit part. It has been noted [3] that the CN/LF method has a smaller truncation error and a larger stability region compared with some other second order methods.

2.2.2 The third order IMEX Runge-Kutta method

The IMEX Runge-Kutta method we consider [2] consists of a four-stage, third order, L-stable, stiffly-accurate, singly diagonally implicit Runge-Kutta method and a four-stage,

third order explicit Runge-Kutta method. We present it in the following form

$$\begin{cases} u^{n,1} = u^n \\ u^{n,s} = u^n + \tau \sum_{l=1}^{s} \tilde{a}_{sl} \mathcal{L}(t_l^n, u^{n,l}) + \tau \sum_{l=1}^{s-1} \hat{a}_{sl} \mathcal{N}(t_l^n, u^{n,l}) \\ u^{n+1} = u^n + \tau \sum_{l=1}^{5} \tilde{b}_l \mathcal{L}(t_l^n, u^{n,l}) + \tau \sum_{l=1}^{5} \hat{b}_l \mathcal{N}(t_l^n, u^{n,l}) \end{cases} , \quad 2 \le s \le 5 , \tag{2.8}$$

where

$$t_l^n = t^n + \tilde{c}_l \tau, \qquad \tilde{c}_s = \sum_{l=2}^{s} \tilde{a}_{sl} = \sum_{l=1}^{s-1} \hat{a}_{sl}. \tag{2.9}$$

Denote $\tilde{A} = (\tilde{a}_{sl}), \hat{A} = (\hat{a}_{sl}) \in \mathbb{R}^{5\times 5}$, $\tilde{b}^T = [\tilde{b}_1, ..., \tilde{b}_5]$ and $\hat{b}^T = [\hat{b}_1, ..., \hat{b}_5]$. Then we can express the time-marching method as the following Butcher tableau

	0	0	0	0	0	0	0	0	0	0	
	0	$\frac{1}{2}$	0	0	0	$\frac{1}{2}$	0	0	0	0	
$\tilde{a}_{sl}$	0	$\frac{1}{6}$	$\frac{1}{2}$	0	0	$\frac{11}{18}$	$\frac{1}{18}$	0	0	0	$\hat{a}_{sl}$
	0	$-\frac{1}{2}$	$\frac{1}{2}$	$\frac{1}{2}$	0	$\frac{5}{6}$	$-\frac{5}{6}$	$\frac{1}{2}$	0	0	
	0	$\frac{3}{2}$	$-\frac{3}{2}$	$\frac{1}{2}$	$\frac{1}{2}$	$\frac{1}{4}$	$\frac{7}{4}$	$\frac{3}{4}$	$-\frac{7}{4}$	0	
$\tilde{b}_l$	0	$\frac{3}{2}$	$-\frac{3}{2}$	$\frac{1}{2}$	$\frac{1}{2}$	$\frac{1}{4}$	$\frac{7}{4}$	$\frac{3}{4}$	$-\frac{7}{4}$	0	$\hat{b}_l$

(2.10)

of which the left half lists $\tilde{a}_{sl}$ and $\tilde{b}_l$, with the five rows from top to bottom corresponding to $s = 1, ..., 5$, and the columns from left to right corresponding to $l = 1, ..., 5$. Similarly, the right half lists $\hat{a}_{sl}$ and $\hat{b}_l$. With the above Butcher coefficients, we then get a third order IMEX Runge-Kutta method.

To identify the EIN methods considered in this paper, if we add and subtract an appropriately large linear term on one side of the equation, and then apply the second order IMEX multi-step method (2.7) to the equivalent equation, then it will be referred to as the EIN-MS2 method. In addition, if apply the third order IMEX Runge-Kutta method (2.8) to the equivalent equation, then it will be referred to as the EIN-RK3 method. To identify the schemes derived in this paper, the EIN-MS2 scheme coupled with the Fourier collocation method will be referred to as the EIN-MS2-FC scheme. When we mention the EIN-RK3-FC

scheme without further clarification, it will be referring to the EIN-RK3 scheme coupled with the Fourier collocation method. In addition, if we replace the Fourier collocation method with the Chebyshev collocation method, we replace the letter "FC" with "CC" accordingly. For example, the EIN-MS2 scheme coupled with the Chebyshev collocation method will be referred to as the EIN-MS2-CC scheme. Sometimes for convenience, we also use the EIN Fourier collocation schemes to refer to both the EIN-MS2-FC and the EIN-RK3-FC schemes. Meanwhile, we use the EIN Chebyshev collocation schemes to refer to both the EIN-MS2-CC and the EIN-RK3-CC schemes.

2.3 Stability analysis

In this subsection we attempt to give stability analysis for the proposed EIN-RK3-FC and EIN-MS2-FC schemes by the aid of the Fourier method. We would like to investigate how to choose a_0 such that the schemes can be stable under the relaxed time step restrictions. The stability analysis of the EIN-RK3-CC and EIN-MS2-CC schemes requires some more complex analytical techniques such as the energy method and will not be presented here. The numerical results obtained in Section 3 indicate that the EIN-RK3-CC and EIN-MS2-CC schemes are also stable provided that the values of a_0 are same with those for the EIN-RK3-FC and EIN-MS2-FC schemes, respectively.

For simplicity of analysis, we consider the simplified linear equation

$$U_t + cU_x = dU_{xx}, \tag{2.11}$$

where $d > 0$ and $c \in \mathbb{R}$. Adding and subtracting a term with constant diffusion coefficient $a_1 U_{xx}$ at the left-hand side of the considered PDE and using the Fourier collocation method to discretize the equation spatially, we can obtain the following system of ordinary differential equations

$$(\tilde{u}_k)_t = \big[(a_1 - d)k^2 - ick\big]\tilde{u}_k - a_1 k^2 \tilde{u}_k, \qquad -N \le k \le N-1, \tag{2.12}$$

where $\tilde{u}_k$ is given by (2.3), $a_1 = a_0 \times d$ and $i^2 = -1$. Coupled with the time-marching

methods, in which the term $\left[(a_1-d)k^2-ick\right]\tilde{u}_k$ is taken as $\mathcal{N}$ and the term $a_1k^2\tilde{u}_k$ is taken as $\mathcal{L}$, we then obtain the fully discrete EIN schemes. Note that if we let $a_0=1$, then the EIN scheme will degenerate to the general IMEX scheme.

2.3.1 The EIN-MS2-FC scheme

Coupled with the EIN-MS2 method (2.7), we can obtain the following characteristic polynomial

$$(1+a_1\tau k^2)z^2+2\tau\left[ick+(d-a_1)k^2\right]z-(1-a_1\tau k^2). \tag{2.13}$$

The stability properties of the scheme are determined by the location of the roots of the characteristic polynomial. Because the L^2 norm of the exact solution to the linear convection-diffusion equation (2.11) does not increase in time, the necessary and sufficient stability condition of the EIN-MS2-FC scheme is given by the following lemma.

Lemma 2.1. *The EIN-MS2-FC scheme is stable if and only if its characteristic polynomial has multiple roots z with $|z|<1$ and simple roots with $|z|\leq 1$.*

Generally, polynomials satisfying the above condition are also called simple von Neumann polynomials. We can reduce the characteristic polynomial to a polynomial of lower degree and use the theory, which originates from Schur [35] and is exposed by Miller in [30], to help us simplify the algebra needed to determine the conditions under which the characteristic polynomial is a simple von Neumann polynomial.

Given a polynomial $\psi(z)=\sum_{j=0}^{s}b_jz^j$ of degree s with $b_0,\,b_s\neq 0$, we can obtain a polynomial $\phi(z)$ of degree $s-1$

$$\phi(z)=\frac{\varphi(0)\psi(z)-\psi(0)\varphi(z)}{z}$$

by introducing $\varphi(z)=\sum_{j=0}^{s}\bar{b}_{s-j}z^j$, where $\bar{b}_{s-j}$ denotes the complex conjugate of b_j. There are two theorems which help us with the stability analysis.

Theorem 2.1. *$\psi(z)$ is a simple von Neumann polynomial if and only if either $|\varphi(0)|>|\psi(0)|$ and $\phi(z)$ is a simple von Neumann polynomial or $\phi(z)\equiv 0$ and $\frac{\mathrm{d}\psi(z)}{\mathrm{d}z}$ is a Schur polynomial.*

Theorem 2.2. *$\psi(z)$ is a Schur polynomial, which has only roots z with $|z| < 1$, if and only if $|\varphi(0)| > |\psi(0)|$ and $\phi(z)$ is a Schur polynomial.*

We use $\psi(z)$ to refer to the characteristic polynomial (2.13) of the EIN-MS2-FC scheme and apply the above two theorems to the scheme. Because $|\varphi(0)| > |\psi(0)|$, $\psi(z)$ is a simple von Neumann polynomial if and only if $\phi(z)$ is, and $\phi(z)$ is given by

$$\phi(z) = 4a_1\tau k^2 z + 4(d - a_1)\tau k^2 + 4ica_1\tau^2 k^3.$$

Therefore, the scheme is stable if and only if

$$(1 - 2a_0) + c^2 a_0^2 k^2 \tau^2 \leq 0.$$

By analyzing the above inequality, we can summarize the results in the following proposition.

Proposition 2.1. *For the linear periodic initial value problem*

$$U_t + cU_x = dU_{xx}, \qquad (x,t) \in \Omega \times [0,\infty), \tag{2.14a}$$

$$U(x,0) = U_0(x), \qquad x \in \Omega, \tag{2.14b}$$

$$U(x + 2\pi, t) = U(x,t), \qquad (x,t) \in \mathbb{R} \times [0,\infty), \tag{2.14c}$$

where $d > 0$, $c \in \mathbb{R}$, $\Omega = [0, 2\pi]$, the EIN-MS2-FC scheme is stable provided that
(1) if $c = 0$ and $a_0 \geq 1/2$, then there are no restrictions on τ;
(2) if $c \neq 0$ and $a_0 > 1/2$, then $0 < \tau \leq \sqrt{2a_0 - 1}/(a_0|c|N)$.

Note that the upper-bound of the time step is independent of the diffusion coefficient d and is related to the size of a_0 in the case of $a_0 > \frac{1}{2}$, $c \neq 0$. In addition, the time step reaches its maximum $\frac{1}{|c|N}$ when $a_0 = 1$.

Remark 2.1. *Note that for the pure convection equation $U_t + cU_x = 0$, $c \in \mathbb{R}$, the Fourier collocation scheme coupled with the Leap-Frog method (the explicit part of the IMEX-MS2 method (2.7)) is stable [25] for $\tau < \frac{1}{|c|N}$. That is, the upper-bound of the time step of the EIN-MS2-FC scheme is less than that of the explicit part of the scheme if $a_0 \neq 1$.*

2.3.2 The EIN-RK3-FC scheme

In this subsection, we analyze the stability of the EIN-RK3-FC scheme for the linear convection-diffusion equation (2.11). We would like to investigate how to choose a_0 such that the scheme can be stable under a relaxed time step restriction. Utilization of the EIN-RK3 method (2.8) to the semi-discrete scheme (2.12) leads to a recurrence relation involving $\tilde{u}_k^n$ and $\tilde{u}_k^{n+1}$

$$\tilde{u}_k^{n+1} = G\tilde{u}_k^n,$$

where the amplification factor G is a scalar function of variables k, c, d, a_0 and is given by

$$G = 1 + G_{\mathcal{N}} \sum_{l=1}^{5} \hat{b}_l M_l + G_{\mathcal{L}} \sum_{l=1}^{5} \tilde{b}_l M_l, \tag{2.15}$$

where

$$\begin{aligned}
&M_1 = 1, \\
&M_s = \left(1 + G_{\mathcal{N}} \sum_{l=1}^{s-1} \hat{a}_{sl} M_l + G_{\mathcal{L}} \sum_{l=1}^{s-1} \tilde{a}_{sl} M_l\right) \Big/ \left(1 - \tilde{a}_{ss} G_{\mathcal{L}}\right), \qquad 2 \le s \le 5, \\
&G_{\mathcal{L}} = -a_0 dk^2, \qquad G_{\mathcal{N}} = (a_0 - 1)dk^2 - ick.
\end{aligned}$$

The specific formulae of $\tilde{a}_{sl}$, $\hat{a}_{sl}, \tilde{b}_l$, $\hat{b}_l$ can be found in (2.10). Because the L^2 norm of the exact solution to the linear convection-diffusion equation (2.11) does not increase in time, the von Neumann stability requires that the magnitude of the amplification factor to be less than or equal to 1, i.e.,

$$|G| \le 1. \tag{2.16}$$

The detailed stability analysis of the EIN-MS3-FC scheme is quite complex. Considering the complexity, we get the stability constraints on τ and a_0 numerically.

We analyze the two cases: $c = 0$ and $c \neq 0$. In the case that $c = 0$, we would like to find the minimum and maximum (if it exists) values of a_0 to assure that the scheme is stable under a relaxed time step restriction. It is preferable that the stability is assured regardless of the time step. On this basis, we then analyze the case of $c \neq 0$, because we usually

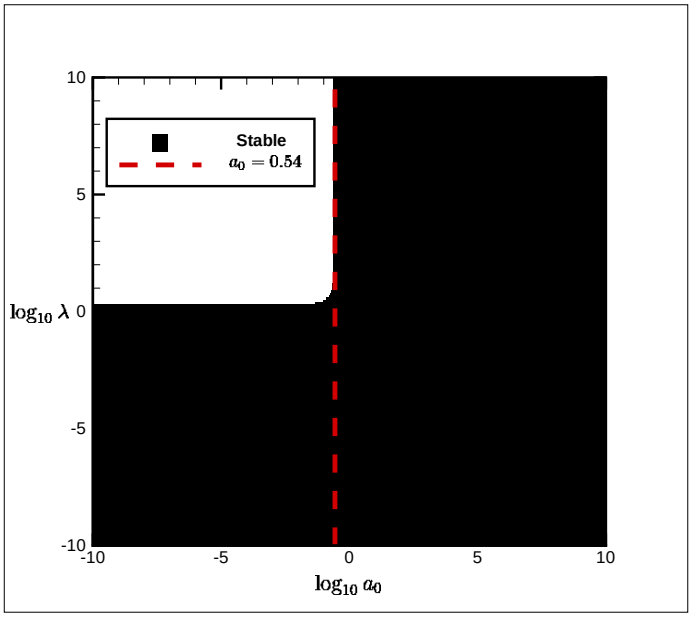

Figure 2.1: *The stability region of the EIN-RK3-FC scheme corresponding to* a_0 *and* λ *for the linear convection-diffusion equation* (2.11) *with* $c = 0$. *The scheme is stable when* a_0 *and* λ *are in the black region.*

cannot expect the stability of the scheme to be better after adding the convection term to the equation.

Taking $c = 0$, the amplification factor G can be simply regarded as a scalar function of the two variables, a_0 and $\lambda = dk^2$. We plot the stability region of the EIN-RK3-FC scheme with $c = 0$ in Figure 2.1 to give an indication of the stability of the scheme. We find that the scheme is unconditionally stable provided that

$$a_0 \geq 0.54,$$

otherwise, the scheme is subject to a strict time step restriction $\tau = O(N^{-2})$ for stability.

Then we analyze the case of $c \neq 0$. For the convection-diffusion equation (2.11), we know that when the local discontinuous Galerkin method is adopted for spatial discretization, the pure IMEX schemes [39] are shown to be stable as long as the time step is upper-bounded by a constant, which depends on the ratio of the diffusion and the square of the convection coefficients and is independent of the mesh size. For the EIN-RK3-FC scheme, we expect to

obtain similar stability, that is, the scheme could be stable under the condition $\tau \leq \tau_0$, where τ_0 is a positive constant depending on the diffusion coefficient d, the convection coefficient c and possibly the stabilization parameter a_0. Next, we would like to explore whether the scheme would allow us to achieve such stability by the Fourier analysis numerically.

During the search for τ_0 we take a sufficiently large integer N in the code. For any fixed a_0, d, c, the values of $|G|$ are computed. By checking whether the inequality (2.16) is satisfied for all k, we can get a range of time step, where k is the frequency and $-N \leq k \leq N-1$. The maximum value of the range is recorded as τ_0. Figure 2.2 shows the maximum time step τ_0 for some choices of a_0. We can see that for any fixed a_0, the scheme is stable as long as the time step is upper-bounded by a positive constant which is proportional to d/c^2, when d/c^2 is relatively small. The approximately linear relationship between τ_0 and d/c^2 can be described as

$$\tau_0 \approx \begin{cases} 0.628\, d/c^2, & a_0 = 0.54, \\ 3.185\, d/c^2, & a_0 = 0.8, \\ 3.893\, d/c^2, & a_0 = 1, \\ 6.35\, d/c^2, & a_0 = 10. \end{cases}$$

When d/c^2 is large, τ_0 is no longer proportional to d/c^2, and when d/c^2 is large enough, the scheme can even be unconditionally stable, which is not shown in the figures. We have calculated the maximum time step of the scheme for a large number of choices of a_0. In general, the gradient of the fitting line increases with the increase of a_0. As a result, the sufficient condition for the stability of the scheme is given by

$$\tau \leq \tau_0 \approx 0.628\, d/c^2.$$

Note that when d/c^2 is very small or even zero, τ_0 would be too small to be the true bound for stability, because the scheme can also be stable under the standard CFL condition

$$N\tau \leq C, \tag{2.17}$$

if the diffusion term is not considered. Next, we would like to further find the possible

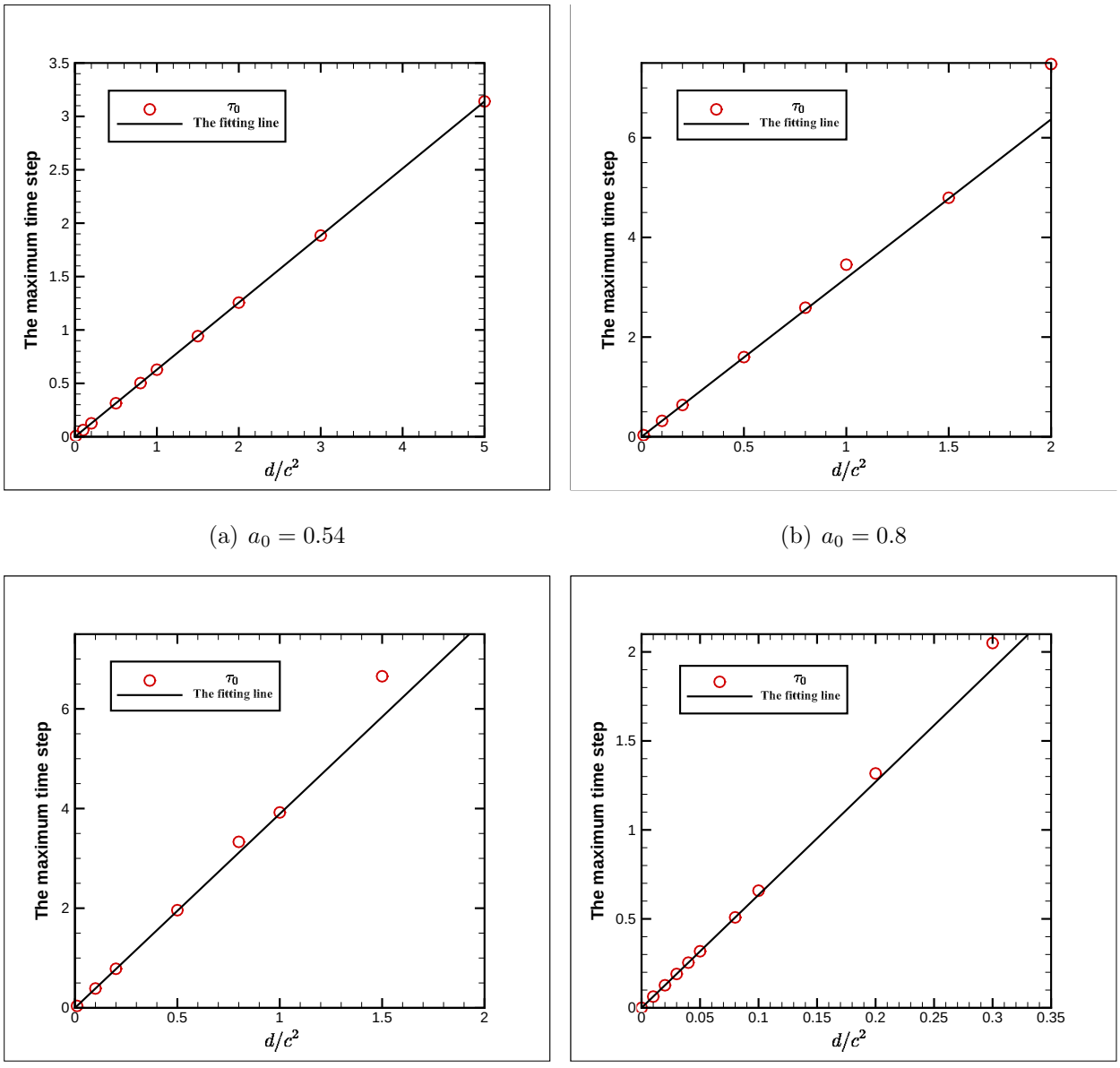

(a) $a_0 = 0.54$

(b) $a_0 = 0.8$

(c) $a_0 = 1$

(d) $a_0 = 10$

Figure 2.2: The maximum time step τ_0 of the EIN-RK3-FC scheme corresponding to the diffusion coefficient d, the convection coefficient c and the stabilization parameter a_0 for the linear convection-diffusion equation (2.11).

CFL-like stability condition for the scheme. Similarly, we obtain the Courant number C in (2.17) numerically. When $d = 0$, we find that no matter what the value of the convection coefficient c is, the scheme is stable for the convection equation $U_t + cU_x = 0$ provided that

$$N\tau \leq 1.56/|c|. \tag{2.18}$$

For each set of $d > 0$, $c \in \mathbb{R}$, the stability of the EIN-RK3-FC scheme for the convection-diffusion equation (2.11) is investigated under the time step (2.18) while a_0 ranges from 0.54 to 1000 in increment of 10^{-2}. The result shows that the scheme can always be stable under the time step (2.18) regardless of the value of a_0. Below we summarize the stability results of the scheme in the following proposition.

Proposition 2.2. *For the linear periodic initial value problem* (2.14)*, the EIN-RK3-FC scheme is stable provided that*

(1) if $c = 0$ *and* $a_0 \geq 0.54$*, then there are no restrictions on* τ*;*

(2) if $c \neq 0$ *and* $a_0 \geq 0.54$*, then* $0 < \tau \leq \max\left\{1.56/(|c|N),\, \tau_0\right\}$*, where* $\tau_0 \approx 0.628\, d/c^2$ *is a constant and* d*,* c *are the diffusion and convection coefficients, respectively.*

3 Numerical experiments

In this section, we will numerically validate the orders of accuracy and performance of the proposed EIN Fourier collocation and EIN Chebyshev collocation schemes for the convection-diffusion equations in one and two space dimensions. In addition, we would like to verify the stability of the proposed numerical schemes in terms of the constant a_1 given in the analysis. The generalization of the Fourier collocation and the Chebyshev collocation method to the two-dimensional equation is straightforward. In the tests, if we use the Fourier collocation method for spatial discretization, the periodic boundary condition is considered, otherwise we consider the Dirichlet-Dirichlet boundary conditions (2.5) given by the exact solution. In the implementation of the EIN-MS2-FC (or the EIN-MS2-CC) scheme, we adopt the EIN-RK3-FC (or the EIN-RK3-CC) scheme to compute the solutions at the first several time levels.

The eigenvalues of the Chebyshev collocation operator associated with the convection term grow like $O(N^2)$, thus, from a stability point of view, we take $\tau = O(N^{-2})$ for all the EIN Chebyshev collocation schemes. As for the EIN Fourier collocation schemes, we take the time step given in the stability analysis.

3.1 The linear numerical test in one dimension

We consider the linear convection-diffusion equation

$$U_t + \underbrace{cU_x - dU_{xx} + a_1 U_{xx}}_{T_1} - \underbrace{a_1 U_{xx}}_{T_2} = 0, \qquad x \in (0, 2\pi) \tag{3.1}$$

augmented with the initial condition $U(x, 0) = \sin(x)$. The problem has an exact solution

$$U(x, t) = e^{-dt} \sin(x - ct). \tag{3.2}$$

We compute to $T = 1$ with the parameter $a_1 = a_0 \times d$ and the coefficients $c = 1, d = 1$. The L^2 errors and orders of the EIN-MS2 and EIN-RK3 schemes in conjunction with the Fourier collocation and Chebyshev collocation methods for this problem are listed in Tables 3.1 and 3.2, respectively. In each table, we display the numerical results of the schemes with different a_0.

From the experiments we can see that all the EIN Fourier collocation schemes are stable and can preserve very nice temporal convergence rates if a_0 is greater than or equal to the stability threshold, while the errors of all the schemes blow up as N increases if a_0 is smaller than the stability threshold. This verifies the stability results produced by our analysis. Please refer to Table 1.1 for the stability threshold of each scheme. We also note that larger a_0 causes larger error. It is normal for this to happen, because the auxiliary term $a_1 U_{xx}$, $a_1 = d \times a_0$ we add to and subtract from the equation are treated in different ways, i.e., one is treated explicitly and the other is treated implicitly. The two different time-stepping methods bring a certain error to the scheme, which increases with the increase of a_0. For this reason, too large a_0 is not recommended.

As illustrated in Table 3.2, the EIN-MS2-CC scheme is stable and can achieve the optimal second order temporal convergence rate if a_0 is greater than the stability threshold, while the errors of all the EIN Chebyshev collocation schemes blow up as N increases if a_0 is smaller than the stability threshold. Since the time step of the EIN Chebyshev collocation schemes is $O(N^{-2})$, compared with the EIN Fourier collocation schemes, the errors of the schemes can easily achieve the machine error with fewer collocation points, and are less sensitive to a_0. In addition, order reduction is observed for the EIN-RK3-CC scheme, that is, the third order temporal convergence rate is not attained and the order of convergence is rather governed by the stage order of the time-marching method (2.8), no matter how dense the mesh grid is. Note that the stage order of the time-marching method (2.8) is 2. Such an order reduction phenomenon results from wrong specifications of intermediate-stage boundary conditions, i.e., we view each intermediate value $u^{n,s}$ in (2.8) as an approximation to $u(t^n + \tilde{c}_s\tau)$, and forces the physical boundary condition at time $t^n + \tilde{c}_s\tau$

$$u^{n,s}(\tilde{x}_0) = g_1(t^n + \tilde{c}_s\tau), \qquad u^{n,s}(\tilde{x}_N) = g_2(t^n + \tilde{c}_s\tau), \qquad 2 \le s \le 5.$$

The specific formulae of $\tilde{c}_s$, $2 \le s \le 5$ can be found in (2.9). For more information about order reduction, please refer to [32, 34, 41]. We adopt a strategy of boundary treatment [41] in Appendix A to help recover the third order convergence rate of the EIN-RK3-CC scheme. The strategy was first proposed to avoid the order reduction when third order IMEX Runge-Kutta time discretization is used together with the local discontinuous Galerkin spatial discretization for solving the convection-diffusion problems with time-dependent Dirichlet-Dirichlet boundary conditions. The results of the EIN-RK3-CC scheme with the boundary treatment (A.3) for the problem (3.1) with Dirichlet-Dirichlet boundary conditions are listed in Table 3.3. As we can see, the smallest a_0 to ensure the stability of the scheme is 0.54. When $a_0 = 10$, the errors are larger and settle down towards the machine error slower with mesh refinements, in comparison with the results of $a_0 = 0.54$ and $a_0 = 1$. Consequently, the optimal order of accuracy can be observed. It further proves the usefulness of the boundary treatment method in retaining the original high order accuracy of the scheme. For

convenience, when we mention the EIN-RK3-CC scheme below without further clarification, it will be referring to the EIN-RK3-CC scheme with the boundary treatment (A.3).

Table 3.1: The errors and orders of the EIN-MS2-FC and EIN-RK3-FC schemes for Example (3.1) with periodic boundary condition.

scheme	τ	N	L^2 error	order	L^2 error	order	L^2 error	order	L^2 error	order
			$a_0 = 0.49$		$a_0 = 0.51$		$a_0 = 1$		$a_0 = 10$	
EIN-MS2-FC	$\frac{\sqrt{\lvert 2a_0-1\rvert}}{a_0 N}$	64	1.63E+04		1.83E-06		4.54E-05		1.15E-04	
		128	1.88E+29	-83.25	4.58E-07	2.00	1.16E-05	1.97	2.89E-05	1.99
		256	1.52E+83	-179.08	1.15E-07	2.00	2.93E-06	1.98	7.26E-06	1.99
		512	NaN	NaN	2.88E-08	2.00	7.36E-07	1.99	1.82E-06	2.00
		1024	NaN	NaN	7.19E-09	2.00	1.84E-07	2.00	4.55E-07	2.00
EIN-RK3-FC	$\frac{1.56}{N}$	64	3.40E-07		3.32E-07		2.95E-07		3.44E-04	
		128	4.40E-08	2.95	4.30E-08	2.95	3.82E-08	2.95	5.26E-05	2.71
		256	5.59E-09	2.98	5.46E-09	2.98	4.86E-09	2.98	7.30E-06	2.85
		512	1.23E+00	-27.71	6.88E-10	2.99	6.12E-10	2.99	9.62E-07	2.92
		1024	2.68E+20	-67.57	8.64E-11	2.99	7.68E-11	2.99	1.24E-07	2.96

3.2 The nonlinear numerical test in one dimension

We consider the nonlinear convection-diffusion equation

$$\underbrace{U_t + \frac{1}{2}(U^2)_x - (d(U)U_x)_x + a_1 U_{xx} - s(x,t)}_{T_1} = \underbrace{a_1 U_{xx}}_{T_2}, \qquad x \in (0, 2\pi) \tag{3.3}$$

augmented with the diffusion coefficient

$$d(U) = 1 + \sigma U^2, \tag{3.4}$$

the initial condition $U(x,0) = \sin(x)$ and the source term

$$s(x,t) = \sin(x+t) - 2\sigma\cos^2(x+t)\sin(x+t) + \sigma\sin^3(x+t) + \cos(x+t)(1+\sin(x+t)).$$

The problem has an exact solution

$$U(x,t) = \sin(x+t).$$

Table 3.2: The errors and orders of the EIN-MS2-CC and EIN-RK3-CC schemes for Example (3.1) with Dirichlet-Dirichlet boundary conditions.

scheme	τ	N	L^2 error	order	L^2 error	order	L^2 error	order	L^2 error	order
			$a_0 = 0.49$		$a_0 = 0.51$		$a_0 = 1$		$a_0 = 10$	
EIN-MS2-CC	$\frac{\sqrt{\lvert 2a_0-1\rvert}}{a_0 N^2}$	16	1.05E-07		1.86E-07		2.34E-06		5.18E-06	
		32	5.96E+36	-72.67	1.18E-08	1.99	1.49E-07	1.98	3.29E-07	1.99
		64	NaN	NaN	7.46E-10	1.99	9.43E-09	1.99	2.08E-08	1.99
		128	NaN	NaN	4.70E-11	1.99	5.92E-10	2.00	1.30E-09	2.00
		256	NaN	NaN	2.65E-12	2.07	3.70E-11	2.00	8.16E-11	2.00
	τ	N	$a_0 = 0.53$		$a_0 = 0.54$		$a_0 = 1$		$a_0 = 10$	
EIN-RK3-CC	$\frac{1.56}{N^2}$	16	5.43E-08		5.60E-08		6.10E-08		9.92E-06	
		32	2.59E-09	2.20	2.78E-09	2.17	3.34E-09	2.10	3.39E-07	2.44
		64	1.34E-10	2.14	1.41E-10	2.15	1.66E-10	2.17	1.56E-08	2.22
		128	7.10E-12	2.12	7.46E-12	2.12	8.69E-12	2.13	7.98E-10	2.14
		256	NaN	NaN	4.62E-13	2.01	5.23E-13	2.03	4.16E-11	2.13

Table 3.3: The errors and orders of the EIN-RK3-CC scheme with the boundary treatment (A.3) for Example (3.1) with Dirichlet-Dirichlet boundary conditions.

τ	N	L^2 error	order	L^2 error	order	L^2 error	order	L^2 error	order
		$a_0 = 0.53$		$a_0 = 0.54$		$a_0 = 1$		$a_0 = 10$	
$\frac{1.56}{N^2}$	16	5.31E-09		5.23E-09		4.80E-09		6.34E-06	
	32	8.59E-11	2.97	8.47E-11	2.97	7.99E-11	2.95	1.12E-07	2.91
	64	1.36E-12	2.99	1.34E-12	2.99	1.30E-12	2.97	1.83E-09	2.97
	128	1.69E-13	1.50	3.18E-14	2.70	6.00E-14	2.22	2.92E-11	2.99
	256	NaN	NaN	2.43E-13	-1.47	2.42E-13	-1.01	3.61E-13	3.17

We compute to $T = 1$ with the stabilization parameter $a_1 = a_0 \times \max_{u^n} d(u^n)$.

First, we test the stability of the proposed schemes for the nonlinear equation in terms of the constant a_0. Tables 3.4 and 3.5 list the L^2 errors and orders of the schemes for (3.3) with the diffusion coefficient $\sigma = 1$. From the experiment we find that the smallest a_0 to ensure the stability of the EIN-MS2-FC and EIN-MS2-CC schemes is 0.51, and the smallest a_0 to ensure the stability of the EIN-RK3-FC scheme is 0.54, which illustrates the sharpness of the threshold values shown in Table 1.1. When $a_0 = 0.53$, although the results of the EIN-RK3-CC scheme do not show any instability phenomenon under the existing mesh, as long as we increase N or decrease the time step, the errors of the scheme will explode. From the numerical results we can also find that larger a_0 may cause larger errors.

Second, we numerically validate the stability and efficiency of the schemes for the nonlinear equation (3.3) with different σ. Since the time step of the EIN-MS2-FC scheme for the linear convection-diffusion equation (2.11) reaches its maximum when $a_0 = 1$, we take $a_0 = 1$ for the EIN-MS2-FC and EIN-MS2-CC schemes in the test. For the EIN-RK3-FC and EIN-RK3-CC schemes, we take $a_0 = 0.54$. Tables 3.6 and 3.7 list the L^2 errors and orders of the schemes for (3.3) with four different diffusion coefficients $\sigma = -1$, 0, 10, 100. It is observed that, all the schemes are stable and the EIN-MS2-FC and EIN-MS2-CC schemes can preserve very nice second order temporal convergence rates with a refined mesh grid regardless of the values of σ. The numerical orders of the EIN-RK3-FC scheme settle down towards the asymptotic value slowly with mesh refinements if σ is large. In addition, larger σ means larger a_1, and it causes larger error. Compared with the EIN-MS2-FC scheme, σ has a more significant impact on the errors of the EIN-RK3-FC scheme. For the EIN-RK3-CC scheme, the expected order of convergence (in time) is obtained, which confirms the usefulness of the strategy of boundary treatment (A.3) in retaining the original high order accuracy of the scheme.

Table 3.4: The errors and orders of the EIN-MS2-FC and EIN-RK3-FC schemes for Example (3.3) with periodic boundary condition.

scheme	τ	N	L^2 error	order	L^2 error	order	L^2 error	order	L^2 error	order
			$a_0 = 0.49$		$a_0 = 0.51$		$a_0 = 1$		$a_0 = 10$	
EIN-MS2-FC	$\frac{\sqrt{\lvert 2a_0-1\rvert}}{a_0 N}$	64	4.20E-02		3.30E-06		8.04E-05		1.53E-04	
		128	4.71E-02	-0.17	8.29E-07	1.99	2.02E-05	1.99	3.82E-05	2.00
		256	NaN	NaN	2.07E-07	2.00	5.06E-06	2.00	9.57E-06	2.00
		512	NaN	NaN	5.18E-08	2.00	1.27E-06	2.00	2.39E-06	2.00
		1024	NaN	NaN	1.30E-08	2.00	3.17E-07	2.00	5.99E-07	2.00
	τ	N	$a_0 = 0.53$		$a_0 = 0.54$		$a_0 = 1$		$a_0 = 10$	
EIN-RK3-FC	$\frac{1.56}{N}$	64	6.95E-07		7.23E-07		3.27E-06		2.64E-03	
		128	8.75E-08	2.99	9.13E-08	2.99	4.42E-07	2.89	4.55E-04	2.53
		256	1.10E-08	2.99	1.15E-08	2.99	5.77E-08	2.94	6.80E-05	2.74
		512	3.67E-06	-8.38	1.44E-09	2.99	7.39E-09	2.97	9.35E-06	2.86
		1024	NaN	NaN	1.81E-10	3.00	9.35E-10	2.98	1.23E-06	2.93

Table 3.5: The errors and orders of the EIN-MS2-CC and EIN-RK3-CC schemes for Example (3.3) with Dirichlet-Dirichlet boundary conditions.

scheme	τ	N	L^2 error	order	L^2 error	order	L^2 error	order	L^2 error	order
			$a_0 = 0.49$		$a_0 = 0.51$		$a_0 = 1$		$a_0 = 10$	
EIN-MS2-CC	$\frac{\sqrt{\lvert 2a_0-1\rvert}}{a_0 N^2}$	16	5.46E-06		5.47E-06		6.32E-06		8.28E-06	
		32	8.55E-09	4.83	8.20E-09	4.86	2.10E-07	2.55	4.14E-07	2.24
		64	5.69E-10	1.99	5.46E-10	1.99	1.40E-08	1.99	2.76E-08	1.99
		128	3.12E-02	-12.99	3.57E-11	1.99	9.03E-10	2.00	1.78E-09	2.00
		256	4.69E-02	-0.30	2.16E-12	2.04	5.78E-11	1.99	1.12E-10	2.01
	τ	N	$a_0 = 0.53$		$a_0 = 0.54$		$a_0 = 1$		$a_0 = 10$	
EIN-RK3-CC	$\frac{1.56}{N^2}$	16	7.11E-05		7.11E-05		7.11E-05		1.06E-04	
		32	1.34E-10	9.85	1.41E-10	9.81	7.13E-10	8.60	9.84E-07	3.50
		64	2.29E-12	3.00	2.40E-12	3.00	1.22E-11	2.99	1.73E-08	2.97
		128	1.94E-13	1.80	9.19E-14	2.38	2.07E-13	2.98	2.86E-10	2.99
		256	8.53E-13	-1.07	7.14E-13	-1.49	1.52E-12	-1.45	5.18E-12	2.91

Table 3.6: The errors and orders of the EIN-MS2-FC and EIN-RK3-FC schemes for Example (3.3) with periodic boundary condition.

scheme	τ	N	L^2 error	order	L^2 error	order	L^2 error	order	L^2 error	order
			$\sigma=-1$		$\sigma=0$		$\sigma=10$		$\sigma=100$	
EIN-MS2-FC	$\frac{1}{N}$	64	8.81E-05		5.37E-05		1.58E-04		4.19E-04	
		128	2.25E-05	1.97	1.35E-05	1.99	3.94E-05	2.01	8.83E-05	2.25
		256	5.65E-06	1.99	3.40E-06	1.99	9.85E-06	2.00	1.87E-05	2.24
		512	1.42E-06	2.00	8.51E-07	2.00	2.46E-06	2.00	4.39E-06	2.09
		1024	3.54E-07	2.00	2.13E-07	2.00	6.15E-07	2.00	1.09E-06	2.01
	τ	N	$\sigma=-1$		$\sigma=0$		$\sigma=10$		$\sigma=100$	
EIN-RK3-FC	$\frac{1.56}{N}$	64	2.34E-06		2.87E-07		1.33E-04		1.17E-02	
		128	3.36E-07	2.80	3.60E-08	3.00	2.14E-05	2.64	3.44E-03	1.77
		256	4.57E-08	2.88	4.50E-09	3.00	3.14E-06	2.77	8.03E-04	2.10
		512	6.02E-09	2.92	5.63E-10	3.00	4.34E-07	2.86	1.56E-04	2.36
		1024	7.76E-10	2.95	7.04E-11	3.00	5.74E-08	2.92	2.64E-05	2.57

Table 3.7: The errors and orders of the EIN-MS2-CC and EIN-RK3-CC schemes for Example (3.3) with Dirichlet-Dirichlet boundary conditions.

scheme	τ	N	L^2 error	order	L^2 error	order	L^2 error	order	L^2 error	order
			$\sigma=-1$		$\sigma=0$		$\sigma=10$		$\sigma=100$	
EIN-MS2-CC	$\frac{1}{N^2}$	16	7.59E-05		1.98E-06		1.75E-05		NaN	
		32	2.42E-07	4.30	1.39E-07	1.99	6.31E-07	2.49	6.91E-06	NaN
		64	1.64E-08	1.98	9.25E-09	1.99	4.20E-08	1.99	3.01E-07	2.31
		128	1.07E-09	1.99	5.98E-10	2.00	2.72E-09	2.00	1.99E-08	1.98
		256	6.86E-11	1.99	3.83E-11	1.99	1.73E-10	2.00	1.27E-09	2.00
	τ	N	$\sigma=-1$		$\sigma=0$		$\sigma=10$		$\sigma=100$	
EIN-RK3-CC	$\frac{1.56}{N^2}$	16	1.17E-04		2.36E-07		5.73E-04		3.24E-01	
		32	3.80E-10	9.44	4.82E-11	6.35	4.17E-08	7.12	1.39E-05	7.52
		64	8.00E-12	2.84	8.21E-13	3.00	7.54E-10	2.95	4.42E-07	2.53
		128	2.98E-13	2.40	1.72E-13	1.14	1.24E-11	2.99	7.43E-09	2.98
		256	1.15E-12	-0.98	8.90E-13	-1.19	8.61E-13	1.94	1.20E-10	2.99

3.3 The nonlinear numerical test in two dimension

We consider the nonlinear convection-diffusion equation in two-dimension

$$\underbrace{U_t+\frac{1}{2}\Big(\big(U^2\big)_x+\big(U^2\big)_y\Big)-\nabla\cdot(d(U)\nabla U)-s(x,y,t)+a_1(U_{xx}+U_{yy})}_{T_1}=\underbrace{a_1(U_{xx}+U_{yy})}_{T_2} \tag{3.5}$$

augmented with the diffusion coefficient (3.4), the initial condition $U(x,y,0)=\sin(x+y)$, $(x,y)\in(0,2\pi)^2$ and the source term

$$\begin{aligned}s(x,y,t)=&\cos(x+y+t)+2\sin(x+y+t)-4\sigma\cos^2(x+y+t)\sin(x+y+t)\\&+2\sigma\sin^3(x+y+t)+\sin\big(2(x+y+t)\big).\end{aligned}$$

The exact solution to the problem is given by

$$U(x,y,t)=\sin(x+y+t). \tag{3.6}$$

We compute to $T=1$ with the diffusion coefficient $\sigma=1$ and the stabilization parameter $a_1=a_0\times\max_{u^n}d(u^n)$. Tables 3.8 and 3.9 list the L^2 errors and orders of the schemes for (3.5) with different a_0. From the experiment we find that the smallest a_0 to ensure the stability of the EIN-MS2-FC and EIN-MS2-CC schemes is 0.51. This time, since the meshes we have used are not refined enough, the results of the EIN-RK3-FC and EIN-RK3-CC schemes have not shown signs of stability deterioration when $a_0=0.53$. In addition, for the EIN-RK3-FC scheme, when $a_0=1$ and $a_0=10$, the errors are larger and the numerical orders of accuracy settle down towards the asymptotic value slower with mesh refinements, in comparison with the results of $a_0=0.54$.

4 Convection-dispersion equation

Consider the convection-dispersion equation (1.2). For such equation, in order to guarantee stability and convergence, the sign of the auxiliary term a_1U_{xxx} we add to both sides of the equation needs to be adjusted according to the sign of $\mathcal{G}'(U_x)$. For example, if $\mathcal{G}'(U_x)>0$ within the whole area Ω, then we should add two equal term with negative dispersion

Table 3.8: The errors and orders of the EIN-MS2-FC and EIN-RK3-FC schemes for Example (3.5) with periodic boundary condition.

scheme	τ	N_x, N_y	L^2 error	order	L^2 error	order	L^2 error	order	L^2 error	order
			$a_0 = 0.49$		$a_0 = 0.51$		$a_0 = 1$		$a_0 = 10$	
EIN-MS2-FC	$\frac{\sqrt{\lvert 2a_0-1\rvert}}{a_0 N_x}$	10	1.58E-04		1.51E-04		3.87E-03		7.57E-03	
		20	1.07E-04	0.56	3.82E-05	1.99	9.69E-04	2.00	1.86E-03	2.03
		40	7.93E-03	-6.22	9.60E-06	1.99	2.43E-04	2.00	4.63E-04	2.00
		80	4.93E-03	0.69	2.41E-06	2.00	6.08E-05	2.00	1.16E-04	2.00
		100	4.42E-03	0.48	1.54E-06	2.00	3.89E-05	2.00	7.42E-05	2.00
	τ	N_x, N_y	$a_0 = 0.53$		$a_0 = 0.54$		$a_0 = 1$		$a_0 = 10$	
EIN-RK3-FC	$\frac{1.56}{N_x}$	10	5.98E-04		6.09E-04		1.47E-03		1.22E-01	
		20	7.90E-05	2.92	8.12E-05	2.91	2.68E-04	2.46	6.00E-02	1.02
		40	1.01E-05	2.97	1.04E-05	2.96	4.37E-05	2.61	2.07E-02	1.54
		80	1.27E-06	2.98	1.33E-06	2.98	6.54E-06	2.74	5.22E-03	1.99
		100	6.53E-07	2.99	6.81E-07	2.98	3.49E-06	2.81	3.16E-03	2.25

Table 3.9: The errors and orders of the EIN-MS2-CC and EIN-RK3-CC schemes for Example (3.5) with Dirichlet-Dirichlet boundary conditions.

scheme	τ	N_x, N_y	L^2 error	order	L^2 error	order	L^2 error	order	L^2 error	order
			$a_0 = 0.49$		$a_0 = 0.51$		$a_0 = 1$		$a_0 = 10$	
EIN-MS2-CC	$\frac{\sqrt{\lvert 2a_0-1\rvert}}{a_0 N_x^2}$	10	6.31E-03		6.32E-03		6.20E-03		6.33E-03	
		20	2.40E-04	2.53	8.27E-08	8.69	1.41E-06	6.48	2.67E-06	6.01
		30	1.91E-03	-2.66	1.17E-08	2.52	2.93E-07	2.02	5.52E-07	2.02
		40	1.51E-03	0.43	3.78E-09	2.02	9.49E-08	2.01	1.79E-07	2.02
		50	7.85E-04	1.49	1.57E-09	2.01	3.94E-08	2.01	7.44E-08	2.01
	τ	N_x, N_y	$a_0 = 0.53$		$a_0 = 0.54$		$a_0 = 1$		$a_0 = 10$	
EIN-RK3-CC	$\frac{1.56}{N_x^2}$	10	7.61E-03		7.61E-03		7.61E-03		8.15E-03	
		20	9.58E-08	8.72	9.57E-08	8.73	1.03E-07	8.67	6.66E-05	3.72
		30	7.40E-10	6.24	7.76E-10	6.18	4.59E-09	4.00	7.20E-06	2.86
		40	1.38E-10	3.00	1.45E-10	3.00	8.65E-10	2.98	1.40E-06	2.92
		50	3.74E-11	3.00	3.92E-11	3.00	2.35E-10	2.99	3.87E-07	2.95

coefficient $-a_1 U_{xxx}, a_1 > 0$ to both sides of the considered equation. Otherwise, the sign of the auxiliary term $a_1 U_{xxx}$ needs to be positive. We only consider the case where the sign of $\mathcal{G}'(U_x)$ is fixed. The discussion of the convection-dispersion equation with the sign of $\mathcal{G}'(U_x)$ varying in space and time is beyond the scope of this work. Assume that $\mathcal{G}'(U_x) > 0$, we add two equal term with constant dispersion coefficient $-a_1 U_{xxx}$ to both sides of the considered equation and get

$$U_t + \underbrace{f(U)_x + \mathcal{G}(U_x)_{xx} - a_1 U_{xxx}}_{T_1} = -\underbrace{a_1 U_{xxx}}_{T_2}, \tag{4.1}$$

where $a_1 = a_0 \times \max_{U_x} |\mathcal{G}'(U_x)|$ and $a_0 > 0$ is a constant to be determined. In this section, we present the Fourier collocation and Chebyshev collocation methods for the convection-diffusion equation (4.1). We still consider the time-marching methods shown in Section 2.2. The Fourier analysis is adopted to explore the stability of the proposed schemes in the linear case.

4.1 The spatial discretizations

4.1.1 The Fourier collocation method

For ease of presentation the spatial period Ω is normalized to $[0, 2\pi]$. Following the notations in Section 2.1.1, the semi-discrete Fourier collocation approximation to the convection-dispersion equation (4.1) with the initial condition (2.1) and periodic boundary condition can be described as follows: find $u_N(t) \in S_N$, such that for x_j, $j = 0, 1, ..., 2N-1$ defined by (2.2), we have

$$u_N(x, 0) = I_N U_0(x),$$

$$\Big\{(u_N)_t + \underbrace{[I_N f(u_N)]_x + \{I_N \mathcal{G}[(u_N)_x]\}_{xx} - a_1 (u_N)_{xxx}}_{T_1}\Big\}(x_j, t) = -\underbrace{a_1 (u_N)_{xxx}}_{T_2}(x_j, t),$$

where I_N is a trigonometric interpolation operator and $I_N U_0 \in S_N$ denotes a trigonometric interpolant of $U_0(x)$ at the Fourier collocation nodes (2.2).

4.1.2 The Chebyshev collocation method

After a suitable mapping normalization, we can assume that the problem is set in the reference space interval $[-1,1]$. Following the notations in Section 2.1.2, we use the Chebyshev collocation method to numerically solve the convection-dispersion equation (4.1) with the initial condition (2.1) and the Dirichlet-Dirichlet-Neumann boundary conditions

$$U(-1,t) = g_1(t), \quad U(1,t) = g_2(t), \quad U_x(1,t) = g_3(t), \qquad 0 \le t \le T. \tag{4.2}$$

Other sets of boundary conditions can be referred to [5,15,33]. The semi-discrete Chebyshev collocation scheme can be defined as follows: seek for a solution $\bar{u}_{N+1}(x,t) \in P_{N+1}$ such that

$$\begin{aligned}
&\Big\{(\bar{u}_{N+1})_t + \underbrace{[I^{\star}_{N+1} f(\bar{u}_{N+1})]_x + \{I^{\star}_{N+1}\mathcal{G}[(\bar{u}_{N+1})_x]\}_{xx} - a_1(\bar{u}_{N+1})_{xxx}}_{T_1}\Big\}(\tilde{x}_j,t) \\
&= -\underbrace{a_1(\bar{u}_{N+1})_{xxx}}_{T_2}(\tilde{x}_j,t), \qquad j = 1,...,N-1,
\end{aligned}$$

and

$$\begin{aligned}
\bar{u}_{N+1}(x,0) &= I^{\star}_{N+1}U_0(x), \\
\bar{u}_{N+1}(-1,t) = g_1(t), \quad \bar{u}_{N+1}(1,t) &= g_2(t), \quad (\bar{u}_{N+1})_x(1,t) = g_3(t),
\end{aligned}$$

where $\tilde{x}_j$ is defined by (2.6). Here, P_{N+1} is the space of algebraic polynomials of degree less than or equal to $N+1$ in $[-1,1]$, and $I^{\star}_{N+1}$ is an interpolation operator satisfying the following conditions

$$\begin{aligned}
I^{\star}_{N+1}U(\tilde{x}_j) &= U(\tilde{x}_j), \qquad j = 0,1,...,N, \\
[I^{\star}_{N+1}U(\tilde{x}_N)]_x &= U_x(\tilde{x}_N).
\end{aligned}$$

The same approach has been also used by Pavoni [33] for the normalized KdV equation.

4.2 Stability analysis

In this subsection we attempt to give stability analysis for the proposed EIN-RK3-FC and EIN-MS2-FC schemes by the aid of the Fourier method. We would like to investigate how

to choose a_0 such that the schemes can be stable under the relaxed time step restrictions. The stability analysis of the EIN-RK3-CC and EIN-MS2-CC schemes for the convection-dispersion equation requires some more complex analytical techniques such as the energy method and will not be presented here. The numerical results obtained in Section 5 indicate that the EIN-RK3-CC and EIN-MS2-CC schemes are also stable provided that the values of a_0 are same with those for the EIN-RK3-FC and EIN-MS2-FC schemes, respectively. Recall that the naming convention of the schemes is given in Section 2.2.2.

For simplicity of analysis, we consider the linear convection-dispersion equation

$$U_t + cU_x + dU_{xxx} = 0, \tag{4.3}$$

where $d > 0$, $c \in \mathbb{R}$. Adding two equal term with constant dispersion coefficient $-a_1 U_{xxx}$ to both sides of (4.3) and adopting the Fourier collocation method to the equivalent equation, we can obtain the following system of ordinary differential equations

$$(\tilde{u}_k)_t = \left[i(d-a_1)k^3 - ick\right]\tilde{u}_k + ia_1k^3\tilde{u}_k, \qquad -N \le k \le N-1, \tag{4.4}$$

where $\tilde{u}_k$ is given by (2.3), $a_1 = a_0 \times d$ and $i^2 = -1$. Coupled with the time-marching methods shown in Section 2.2, in which the term $\left[i(d-a_1)k^3 - ick\right]\tilde{u}_k$ is taken as $\mathcal{N}$ and the term $ia_1k^3\tilde{u}_k$ is taken as $\mathcal{L}$, we then obtain the fully discrete schemes. Note that $a_1 = d \times a_0$, and if we let $a_0 = 1$, the EIN scheme will degenerate to the general IMEX scheme.

4.2.1 The EIN-MS2-FC scheme

Coupled with the EIN-MS2 method (2.7), we can obtain the following characteristic polynomial

$$\psi(z) = (1 - ia_0d\tau k^3)z^2 + 2i\tau\left[ck - d(1-a_0)k^3\right]z - (1 + ia_0d\tau k^3).$$

Because the L^2 norm of the exact solution to the linear convection-dispersion equation (4.3) does not increase in time, stability requires the characteristic polynomial to be a simple von Neumann polynomial, which has no roots z with $|z| > 1$ and only simple roots with $|z| = 1$.

Considering the theorems 2.1 and 2.2, because $|\varphi(0)| = |\psi(0)|$ and $\phi(z) \equiv 0$, $\psi(z)$ is a simple von Neumann polynomial if and only if $\frac{\mathrm{d}\psi(z)}{\mathrm{d}z}$ is a Schur polynomial, which demands that

$$k^2\tau^2\left[c^2 - 2cd(1-a_0)k^2 + d^2(1-2a_0)k^4\right] < 1, \qquad -N \le k \le N-1.$$

The above inequality is trivially satisfied for $k = 0$, so that we only need to consider the inequality for $|k| = 1$ to $|k| = N$. By analyzing the above inequality, we can summarize the results in the following proposition.

Proposition 4.1. *For the linear periodic initial value problem*

$$U_t + cU_x + dU_{xxx} = 0, \qquad (x,t) \in \Omega \times [0,\infty), \tag{4.5a}$$

$$U(x,0) = U_0(x), \qquad x \in \Omega, \tag{4.5b}$$

$$U(x+2\pi,t) = U(x,t), \qquad (x,t) \in \mathbb{R} \times [0,\infty), \tag{4.5c}$$

where $\Omega = [0,2\pi]$, $d > 0$, $c \in \mathbb{R}$, *the EIN-MS2-FC scheme is stable provided that*

(1) *if* $a_0 < \frac{1}{2}$ *and* $N^2 \ge \frac{2c(1-a_0)}{d(1-2a_0)}$, *then* $\tau^2 < \frac{1}{N^2\left[d^2(1-2a_0)N^4 - 2cd(1-a_0)N^2 + c^2\right]}$;

(2) *if* $a_0 < \frac{1}{2}$ *and* $N^2 < \frac{2c(1-a_0)}{d(1-2a_0)}$, *then* $\tau^2 \le \frac{1}{N^2c^2}$;

(3) *if* $a_0 = \frac{1}{2}$ *and* $c < 0$, *then* $\tau^2 < \frac{1}{N^2(c^2 - dcN^2)}$;

(4) *if* $a_0 = \frac{1}{2}, c > 0$ *and* $\frac{c^2}{dc} \le 1$, *then there are no restrictions on* τ;

(5) *if* $a_0 = \frac{1}{2}, c > 0$ *and* $\frac{c^2}{dc} > 1$, *then* $\tau^2 \le \frac{dc}{c^2(c^2 - dc)}$;

(6) *if* $a_0 \ge \frac{1}{2}$ *and* $c = 0$, *then there are no restrictions on* τ;

(7) *if* $a_0 > \frac{1}{2}$ *and* $\frac{c(1-a_0) - |c|a_0}{d(1-2a_0)} \le 1$, *then there are no restrictions on* τ;

(8) *if* $a_0 > \frac{1}{2}, \frac{c(1-a_0) - |c|a_0}{d(1-2a_0)} > 1$ *and* $c(1-a_0) \ge 0$, *then*

$$\tau^2 \le \frac{d(1-2a_0)}{\left[d^2(1-2a_0) - 2dc(1-a_0) + c^2\right]\left[c(1-a_0) - |c|a_0\right]};$$

(9) *if* $a_0 > \frac{1}{2}, \frac{c(1-a_0) - |c|a_0}{d(1-2a_0)} > 1$ *and* $c(1-a_0) < 0$, *then* $\tau^2 \le \frac{d(2a_0-1)^2}{a_0^2c^2\left[|c|a_0 - c(1-a_0)\right]}$.

The result shows that the EIN-MS2-FC scheme will be subject to a strict time step $O(N^{-2})$ for stability, if $a_0 = \frac{1}{2}$ and $c < 0$. When $a_0 > \frac{1}{2}$, the EIN-MS2-FC scheme can always be stable for the linear convection-dispersion equation (4.3) as long as the time step is upper-bounded by a positive constant, which depends on the dispersion coefficient d, the convection coefficient c and the stabilization parameter a_0. It is a much weaker condition than the standard CFL condition. Also, note that for the pure convection equation $U_t + cU_x = 0$, $c \in \mathbb{R}$, the Fourier collocation scheme coupled with the Leap-Frog method (the explicit part of the IMEX-MS2 method (2.7)) is stable [25] for $\tau < \frac{1}{|c|N}$.

4.2.2 The EIN-RK3-FC scheme

In this subsection, we analyze the stability of the EIN-RK3-FC scheme for the linear convection-dispersion equation (4.3). We would like to investigate how to choose a_0 such that the scheme can be stable under a relaxed time step restriction. Utilization of the EIN-RK3 method (2.8) to the semi-discrete scheme (4.4) leads to an amplification factor G of the form (2.15), where

$$G_{\mathcal{L}} = ia_0dk^3, \qquad G_{\mathcal{N}} = id(1-a_0)k^3 - ick.$$

Because the L^2 norm of the exact solution to the linear convection-dispersion equation (4.3) does not increase in time, the von Neumann stability requires the amplification factor to meet the condition (2.16). The detailed stability analysis of the scheme is quite complex. Considering the complexity, similar stability analysis method of the EIN-RK3-FC scheme for the linear convection-diffusion equation (2.11) can be applied to analyze the EIN-RK3-FC scheme for the linear convection-dispersion equation (4.3). We omit the full analysis process because of the similarity and summarize the stability results of the scheme in the following proposition.

Proposition 4.2. *For the linear periodic initial value problem* (4.5)*, the EIN-RK3-FC scheme is stable provided that*

(1) if $c = 0$ *and* $a_0 \geq 0.54$*, then there are no restrictions on* τ*;*

(2) if $c \neq 0$ *and* $a_0 \geq 0.54$*, then* $0 < \tau \leq \max\{1.56/(|c|N), \tau_0\}$*, where* τ_0 *is a constant depending on* a_0*,* d*,* c*.*

The result shows that the stability criteria of the EIN-RK3-FC scheme for the linear convection-dispersion equation (4.3) are almost the same as those of the EIN-RK3-FC scheme for the linear convection-diffusion equation (2.11). It is worth mentioning that for the linear convection-dispersion equation (4.3), the linear dependency between τ_0 and d/c^2 does not hold any more when a_0 is fixed. We have calculated the maximum time step of the scheme for a large number of choices of a_0, d, c, however, we cannot generalize the relationship between the constant τ_0 and a_0, d, c with expressions.

5 Numerical experiments

In this section, we will numerically validate the orders of accuracy and performance of the proposed EIN Fourier collocation and EIN Chebyshev collocation schemes for the convection-dispersion equations in one and two space dimensions. In addition, we would like to verify the stability of the proposed schemes in terms of the constant a_1 given in the analysis. The generalization of the Fourier collocation and the Chebyshev collocation method to the two-dimensional equation is straightforward. In the tests, if we use the Fourier collocation method for spatial discretization, the periodic boundary condition is considered, otherwise we consider the Dirichlet-Dirichlet-Neumann boundary conditions (4.2) given by the exact solution. For the EIN-RK3-CC scheme, we use the strategy of boundary treatment (A.3) to deal with the Dirichlet-Dirichlet-Neumann boundary conditions, unless otherwise stated. In the implementation of the EIN-MS2-FC (or the EIN-MS2-CC) scheme, we adopt the EIN-RK3-FC (or the EIN-RK3-CC) scheme to compute the solutions at the first several time levels. Since the eigenvalues of the Chebyshev collocation operator associated with the convection term grow like $O(N^2)$, from a stability point of view, we take $\tau = O(N^{-2})$ for all the EIN Chebyshev collocation schemes. As for the EIN Fourier collocation schemes, we

take the time step given in the stability analysis.

5.1 The linear numerical test in one dimension

First we compute the linear convection-dispersion equation

$$U_t + \underbrace{cU_x + dU_{xxx} - a_1 U_{xxx}}_{T_1} + \underbrace{a_1 U_{xxx}}_{T_2} = 0, \qquad x \in (0, 2\pi) \tag{5.1}$$

augmented with the initial condition $U(x,0) = \sin(x)$. The exact solution is given by

$$U(x,t) = \sin\big(x + (d-c)t\big).$$

The numerical errors and orders of accuracy are measured at $T = \pi$ with the stabilization parameter $a_1 = a_0 \times d$ and the coefficients $d = 2$, $c = -1$. In Tables 5.1 and 5.2, we list the numerical results of the EIN-MS2 and EIN-RK3 schemes in conjunction with the Fourier collocation and Chebyshev collocation methods for this example with different a_0. From these two tables we can see that the smallest a_0 to ensure the stability of the EIN-MS2-FC and EIN-MS2-CC schemes is 0.51, and the smallest a_0 to ensure the stability of the EIN-RK3-FC and EIN-RK3-CC scheme is 0.54, which illustrates the sharpness of the threshold values shown in Table 1.1. From the results we can also find that larger a_0 may cause larger error. In addition, owing to the time step of $O(N^{-2})$, the errors of the EIN Chebyshev collocation schemes can easily achieve the machine error with fewer collocation points, and are less sensitive to a_0 compared with the EIN Fourier collocation schemes.

5.2 The nonlinear numerical test in one dimension

We consider the nonlinear convection-dispersion equation

$$U_t + \underbrace{(\frac{U^2}{2})_x + U_{xxx} + \sigma(U_x^3)_{xx} - a_1 U_{xxx} - s(x,t)}_{T_1} + \underbrace{a_1 U_{xxx}}_{T_2} = 0, \qquad x \in (0, 2\pi) \tag{5.2}$$

augmented with the initial condition $U(x,0) = \cos(x)$ and the source term

$$s(x,t) = -\frac{1}{2}(3\sigma + 2\cos(x+t) + 9\sigma\cos(2(x+t)))\sin(x+t).$$

Table 5.1: The errors and orders of the EIN-MS2-FC and EIN-RK3-FC schemes for Example (5.1) with periodic boundary condition.

scheme	τ	N	L^2 error	order	L^2 error	order	L^2 error	order	L^2 error	order
			$a_0 = 0.5$		$a_0 = 0.51$		$a_0 = 1$		$a_0 = 10$	
EIN-MS2-FC	$\frac{1}{N}$	64	4.31E-05		4.84E-05		2.43E-03		4.54E-02	
		128	1.27E+00	-14.85	1.21E-05	2.00	6.07E-04	2.00	1.15E-02	1.98
		256	6.40E+06	-22.26	3.04E-06	2.00	1.52E-04	2.00	2.89E-03	1.99
		512	2.20E+16	-31.68	7.61E-07	2.00	3.81E-05	2.00	7.23E-04	2.00
		1024	4.22E+29	-44.13	1.90E-07	2.00	9.52E-06	2.00	1.81E-04	2.00
	τ	N	$a_0 = 0.53$		$a_0 = 0.54$		$a_0 = 1$		$a_0 = 10$	
EIN-RK3-FC	$\frac{1.56}{N}$	64	4.39E-05		4.29E-05		3.23E-05		5.89E-02	
		128	1.53E+01	-18.42	5.43E-06	2.98	4.09E-06	2.98	7.77E-03	2.92
		256	4.89E+16	-51.50	6.83E-07	2.99	5.15E-07	2.99	9.91E-04	2.97
		512	1.31E+48	-104.40	8.57E-08	2.99	6.46E-08	2.99	1.25E-04	2.99
		1024	1.34E+111	-209.31	1.07E-08	3.00	8.09E-09	3.00	1.56E-05	3.00

Table 5.2: The errors and orders of the EIN-MS2-CC and EIN-RK3-CC schemes for Example (5.1) with Dirichlet-Dirichlet-Neumann boundary conditions.

scheme	τ	N	L^2 error	order	L^2 error	order	L^2 error	order	L^2 error	order
			$a_0 = 0.5$		$a_0 = 0.51$		$a_0 = 1$		$a_0 = 10$	
EIN-MS2-CC	$\frac{1}{N^2}$	16	3.12E+00		2.75E-07		1.38E-05		2.62E-04	
		32	1.90E+03	-4.62	1.70E-08	2.01	8.49E-07	2.01	1.61E-05	2.01
		64	2.57E+31	-46.72	1.05E-09	2.01	5.26E-08	2.01	1.00E-06	2.01
		128	2.36E+93	-102.92	6.56E-11	2.00	3.28E-09	2.00	6.23E-08	2.00
		256	NaN	NaN	4.41E-12	1.95	2.04E-10	2.00	3.88E-09	2.00
	τ	N	$a_0 = 0.53$		$a_0 = 0.54$		$a_0 = 1$		$a_0 = 10$	
EIN-RK3-CC	$\frac{1.56}{N^2}$	16	1.20E-07		1.11E-07		8.65E-08		1.77E-04	
		32	2.04E+106	-188.07	1.70E-09	3.01	1.36E-09	3.00	3.44E-06	2.84
		64	NaN	NaN	2.59E-11	3.02	2.08E-11	3.01	5.81E-08	2.94
		128	NaN	NaN	1.80E-12	1.92	1.88E-12	1.73	9.49E-10	2.97
		256	NaN	NaN	1.92E-12	-0.04	1.96E-12	-0.03	1.64E-11	2.93

The exact solution to the problem is defined by

$$U(x,t) = \cos(x+t).$$

First, we test the stability of the proposed schemes for the nonlinear equation in terms of the constant a_0. We compute to $T = \pi$ with the coefficient $\sigma = 1$ and the stabilization parameter $a_1 = a_0 \times (1 + 3\max_{u^n}(u^n)^2)$. Tables 5.3 and 5.4 list the L^2 errors and orders of the schemes for (5.2) with different a_0. From the numerical results we can find that the the EIN-MS2-FC and EIN-MS2-CC schemes remain stable as always if $a_0 \geq 0.51$, and the smallest a_0 to ensure the stability of the EIN-RK3-FC and EIN-RK3-CC schemes is 0.54. For the EIN-RK3-CC scheme, the expected order of convergence (in time) is obtained, which confirms the usefulness of the strategy of boundary treatment in retaining the original high order accuracy of the scheme.

Second, we numerically validate the stability and efficiency of the schemes for the nonlinear equation (5.2) with different dispersion coefficients. In the test, we take $a_1 = (1 + 3\sigma\max_{u_x^n}(u_x^n)^2)$ for the EIN-MS2-FC and EIN-MS2-CC schemes. For the EIN-RK3-FC and EIN-RK3-CC schemes, we take $a_1 = 0.54(1 + 3\sigma\max_{u_x^n}(u_x^n)^2)$. We compute to $T = 1$ with four different dispersion coefficients $\sigma = -0.33$, 0, 1, 10. Tables 5.5 and 5.6 list the L^2 errors and orders of the schemes for (5.2) with different σ. It is observed that, all the schemes are stable and the EIN-MS2-FC and EIN-MS2-CC schemes can preserve very nice second order temporal convergence rates as N increases regardless of the values of σ. Larger σ also means larger a_1, and it will bring larger error. Thus, when $\sigma = 10$, the errors of the EIN-RK3-FC scheme are much larger and the numerical orders of accuracy settle down towards the asymptotic value much slower with mesh refinements, in comparison with the results of $\sigma = 0$.

Table 5.3: The errors and orders of the EIN-MS2-FC and EIN-RK3-FC schemes for Example (5.2) with periodic boundary condition.

scheme	τ	N	L^2 error	order	L^2 error	order	L^2 error	order	L^2 error	order
			$a_0 = 0.5$		$a_0 = 0.51$		$a_0 = 1$		$a_0 = 10$	
EIN-MS2-FC	$\frac{1}{N}$	64	1.54E-04		1.61E-04		3.38E-04		3.68E-03	
		128	3.79E-05	2.03	3.83E-05	2.07	8.34E-05	2.02	9.11E-04	2.02
		256	9.49E-06	2.00	9.65E-06	1.99	2.09E-05	2.00	2.27E-04	2.01
		512	2.37E-06	2.00	2.42E-06	1.99	5.22E-06	2.00	5.65E-05	2.00
		1024	5.94E-07	2.00	6.07E-07	2.00	1.31E-06	2.00	1.41E-05	2.00
	τ	N	$a_0 = 0.53$		$a_0 = 0.54$		$a_0 = 1$		$a_0 = 10$	
EIN-RK3-FC	$\frac{1.56}{N}$	64	4.86E-05		4.96E-05		1.48E-04		5.27E-02	
		128	4.87E-05	0.00	7.28E-06	2.77	3.06E-05	2.27	2.75E-02	0.94
		256	4.70E-05	0.05	9.71E-07	2.91	5.17E-06	2.57	4.57E-03	2.59
		512	3.60E-05	0.38	1.29E-07	2.92	7.11E-07	2.86	6.21E-04	2.88
		1024	2.79E-05	0.37	1.64E-08	2.97	9.17E-08	2.96	8.13E-05	2.93

Table 5.4: The errors and orders of the EIN-MS2-CC and EIN-RK3-CC schemes for Example (5.2) with Dirichlet-Dirichlet-Neumann boundary conditions.

scheme	τ	N	L^2 error	order	L^2 error	order	L^2 error	order	L^2 error	order
			$a_0 = 0.5$		$a_0 = 0.51$		$a_0 = 1$		$a_0 = 10$	
EIN-MS2-CC	$\frac{1}{N^2}$	16	8.78E+01		4.01E+02		5.13E-01		1.48E-04	
		32	3.83E-07	13.89	3.93E-07	14.96	8.42E-07	9.61	9.11E-06	2.01
		64	2.38E-08	2.00	2.43E-08	2.01	5.23E-08	2.00	5.66E-07	2.00
		128	1.48E-09	2.00	1.52E-09	2.00	3.26E-09	2.00	3.52E-08	2.00
		256	9.25E-11	2.00	9.47E-11	2.00	2.03E-10	2.00	2.20E-09	2.00
	τ	N	$a_0 = 0.53$		$a_0 = 0.54$		$a_0 = 1$		$a_0 = 10$	
EIN-RK3-CC	$\frac{1.56}{N^2}$	16	5.55E-07		5.57E-07		1.23E-06		7.62E-04	
		32	4.19E-09	3.52	4.41E-09	3.49	2.39E-08	2.85	1.73E-05	2.73
		64	2.66E-07	-3.00	7.17E-11	2.97	3.94E-10	2.96	3.19E-07	2.88
		128	4.14E-07	-0.32	2.68E-12	2.37	7.79E-12	2.83	5.30E-09	2.96
		256	1.26E-06	-0.80	2.95E-12	-0.07	3.08E-12	0.67	8.81E-11	2.96

Table 5.5: The errors and orders of the EIN-MS2-FC and EIN-RK3-FC schemes for Example (5.2) with periodic boundary condition.

scheme	τ	N	L^2 error	order	L^2 error	order	L^2 error	order	L^2 error	order
			$\sigma=-0.33$		$\sigma=0$		$\sigma=1$		$\sigma=10$	
EIN-MS2-FC	$\frac{1}{N}$	64	5.81E-05		5.58E-05		2.71E-04		3.41E-04	
		128	1.56E-05	1.89	1.42E-05	1.98	6.91E-05	1.97	6.43E-05	2.41
		256	4.13E-06	1.92	3.57E-06	1.99	1.74E-05	1.99	1.00E-05	2.68
		512	1.04E-06	1.99	8.96E-07	1.99	4.38E-06	1.99	2.03E-06	2.30
		1024	2.60E-07	2.00	2.24E-07	2.00	1.10E-06	2.00	4.68E-07	2.11
	τ	N	$\sigma=-0.33$		$\sigma=0$		$\sigma=1$		$\sigma=10$	
EIN-RK3-FC	$\frac{1.56}{N}$	64	3.96E-07		9.08E-08		1.64E-05		2.62E-04	
		128	6.72E-08	2.56	1.12E-08	3.02	2.22E-06	2.88	5.67E-05	2.21
		256	1.05E-08	2.68	1.40E-09	3.00	2.90E-07	2.94	9.43E-06	2.59
		512	1.50E-09	2.80	1.74E-10	3.00	3.76E-08	2.95	1.72E-06	2.45
		1024	2.01E-10	2.90	2.18E-11	3.00	4.72E-09	3.00	2.62E-07	2.71

Table 5.6: The errors and orders of the EIN-MS2-CC and EIN-RK3-CC schemes for Example (5.2) with Dirichlet-Dirichlet-Neumann boundary conditions.

scheme	τ	N	L^2 error	order	L^2 error	order	L^2 error	order	L^2 error	order
			$\sigma=-0.33$		$\sigma=0$		$\sigma=1$		$\sigma=10$	
EIN-MS2-CC	$\frac{1}{N^2}$	16	3.99E-06		4.73E-07		3.90E-05		3.41E-05	
		32	NaN	NaN	2.92E-08	2.01	4.26E-07	3.26	2.13E-06	2.00
		64	1.20E-04	NaN	1.81E-09	2.00	2.65E-08	2.00	1.32E-07	2.00
		128	4.21E-06	2.41	1.13E-10	2.00	1.65E-09	2.00	8.25E-09	2.00
		256	1.03E-08	4.34	7.21E-12	1.98	1.03E-10	2.00	5.14E-10	2.00
	τ	N	$\sigma=-0.33$		$\sigma=0$		$\sigma=1$		$\sigma=10$	
EIN-RK3-CC	$\frac{1.56}{N^2}$	16	1.61E-06		2.71E-09		9.55E-07		2.64E-05	
		32	1.84E-10	6.55	2.82E-11	3.29	2.34E-09	4.34	1.02E-06	2.34
		64	3.02E-12	2.96	4.13E-13	3.05	3.90E-11	2.95	2.87E-08	2.58
		128	8.53E-14	2.57	2.05E-13	0.50	6.63E-13	2.94	5.50E-10	2.85
		256	2.49E-13	-0.77	1.92E-12	-1.61	2.52E-13	0.70	8.92E-12	2.97

5.2.1 The nonlinear numerical test in two dimension

We solve the Zakharov-Kuznetsov (ZK) equation [19] in two-dimension

$$U_t + \underbrace{\left(\frac{U^2}{2}\right)_x + U_{xxx} + U_{xyy} - a_1\left(U_{xxx} + U_{xyy}\right) - s(x,y,t)}_{T_1} + \underbrace{a_1\left(U_{xxx} + U_{xyy}\right)}_{T_2} = 0 \qquad (5.3)$$

augmented with the initial condition $U(x,y,0) = \sin(x+y)$, $(x,y) \in (0,2\pi)^2$ and the source term

$$s(x,y,t) = \cos(x+y+t)\left(-1 + \sin(x+y+t)\right).$$

The exact solution is given by (3.6). To avoid ambiguity, we give the Dirichlet-Dirichlet-Neumann boundary conditions as follows:

$$\begin{aligned} U(0,y,t) &= \sin(y+t), & U(2\pi,y,t) &= \sin(2\pi+y+t), \\ U_x(2\pi,y,t) &= \cos(2\pi+y+t), & U(x,0,t) &= \sin(x+t), \\ U(x,2\pi,t) &= \sin(x+2\pi+t). \end{aligned}$$

The numerical errors and orders of accuracy are measured at $T = \pi$ with the stabilization parameter $a_1 = a_0$. In Tables 5.5 and 5.6, we present the numerical results of the schemes with different a_0. As one can see, all the schemes remain stable as always if a_0 is greater than or equal to the stability threshold, while the simulation of the schemes deteriorates significantly with mesh refinements if a_0 is smaller than the stability threshold shown in Table 1.1. Also, larger a_0 brings larger errors. Owing to the time step of $O(N^{-2})$, the deterioration of the errors of the EIN Chebyshev collocation schemes is less severe than that of the EIN Fourier collocation schemes with the same a_0. The numerical results are in good agreement with the theory.

6 Concluding remarks

We have considered the Fourier collocation and Chebyshev collocation schemes coupled with two specific high order explicit-implicit-null time-marching methods for solving the

Table 5.7: The errors and orders of the EIN-MS2-FC and EIN-RK3-FC schemes for Example (5.3) with periodic boundary condition.

scheme	τ	N_x, N_y	L^2 error	order	L^2 error	order	L^2 error	order	L^2 error	order
			$a_0 = 0.5$		$a_0 = 0.51$		$a_0 = 1$		$a_0 = 10$	
EIN-MS2-FC	$\frac{1}{N_x}$	20	3.80E-03		1.26E-03		3.04E-03		3.63E-02	
		40	5.82E-03	-0.62	3.14E-04	2.00	7.64E-04	1.99	8.95E-03	2.02
		60	1.11E-02	-1.60	1.40E-04	1.99	3.39E-04	2.00	4.02E-03	1.98
		80	2.24E-02	-2.43	7.86E-05	2.01	1.91E-04	2.00	2.25E-03	2.01
		100	2.55E-01	-10.91	5.04E-05	1.99	1.22E-04	2.00	1.44E-03	2.01
	τ	N_x, N_y	$a_0 = 0.53$		$a_0 = 0.54$		$a_0 = 1$		$a_0 = 10$	
EIN-RK3-FC	$\frac{1.56}{N_x}$	20	5.91E-05		6.13E-05		1.47E-04		1.57E-01	
		40	7.46E-06	2.99	7.73E-06	2.99	1.78E-05	3.04	5.50E-02	1.52
		60	2.23E-06	2.98	2.30E-06	2.99	5.22E-06	3.02	1.89E-02	2.64
		80	7.43E-05	-12.19	9.71E-07	2.99	2.19E-06	3.02	8.34E-03	2.84
		100	4.43E-02	-28.63	4.97E-07	3.00	1.12E-06	3.01	4.35E-03	2.91

Table 5.8: The errors and orders of the EIN-MS2-CC and EIN-RK3-CC schemes for Example (5.3) with Dirichlet-Dirichlet-Neumann boundary conditions.

scheme	τ	N_x, N_y	L^2 error	order	L^2 error	order	L^2 error	order	L^2 error	order
			$a_0 = 0.5$		$a_0 = 0.51$		$a_0 = 1$		$a_0 = 10$	
EIN-MS2-CC	$\frac{1}{N_x^2}$	10	4.43E-01		3.50E-04		2.53E-04		6.43E-04	
		20	NaN	NaN	1.18E-06	4.11	2.86E-06	3.23	3.38E-05	2.13
		30	NaN	NaN	2.29E-07	2.02	5.55E-07	2.02	6.55E-06	2.02
		40	NaN	NaN	7.17E-08	2.02	1.74E-07	2.02	2.05E-06	2.02
		50	NaN	NaN	2.92E-08	2.01	7.09E-08	2.01	8.37E-07	2.01
	τ	N_x, N_y	$a_0 = 0.53$		$a_0 = 0.54$		$a_0 = 1$		$a_0 = 10$	
EIN-RK3-CC	$\frac{1.56}{N_x^2}$	10	2.44E-04		2.44E-04		2.44E-04		1.13E-03	
		20	1.15E+00	-6.10	2.39E-09	8.32	5.83E-09	7.68	1.97E-05	2.92
		30	NaN	NaN	2.09E-10	3.01	5.12E-10	3.00	1.78E-06	2.96
		40	NaN	NaN	3.95E-11	2.90	9.65E-11	2.90	3.22E-07	2.97
		50	NaN	NaN	4.60E-11	-0.35	8.39E-11	0.31	8.51E-08	2.98

convection-diffusion and convection-dispersion equations in one and two space dimensions. We have presented the stability analysis of the proposed EIN Fourier collocation schemes for the one-dimensional simplified linear equations, and through the analysis we show that the resulting schemes are stable with particular emphasis on the use of large time steps if appropriate stabilization parameters a_1 are chosen. To verify the correctness of the result, a number of numerical tests including one-dimensional and two-dimensional linear and nonlinear problems have been considered. Numerical experiments show that the schemes are stable and can achieve optimal orders of accuracy if the constraints presented in Table 1.1 are satisfied. while the simulation results deteriorate significantly if the constraints are violated. Even though the analysis is only performed on the EIN Fourier collocation schemes, numerical experiments show that the stability criteria can also be extended to the EIN Chebyshev collocation schemes. In the future, we would like to explore the stability of the EIN schemes coupled with the local discontinuous Galerkin methods for the high order dissipative and dispersive equations with variable coefficients.

References

[1] L. Abia and J. M. Sanz-Serna, *The spectral accuracy of a fully-discrete scheme for a nonlinear third order equation*, Computing, 44, 1990, 187-196.

[2] U. M. Ascher, S. J. Ruuth and R. J. Spiteri, *Implicit-explicit Runge-Kutta methods for time-dependent partial differential equations*, Applied Numerical Mathematics, 25, 1997, 151-167.

[3] U. M. Ascher, S. J. Ruuth and B. T. R. Wetton, *Implicit-explicit methods for time-dependent partial differential equations*, SIAM Journal on Numerical Analysis, 32, 1995, 797-823.

[4] F. Bassi, L. Botti, A. Colombo, A. Ghidoni and F. Massa, *Linearly implicit Rosenbrock-type Runge-Kutta schemes applied to the Discontinuous Galerkin solution of compressible and incompressible unsteady flows*, Computers and Fluids, 118, 2015, 305-320.

[5] J. L. Bona, S. M. Sun and B.-Y. Zhang, *A nonhomogeneous boundary-value problem for the Korteweg-de Vries equation posed on a finite domain*, Journal of Differential Equations, 28, 2003, 1391-1436.

[6] N. Bressan and A. Quarteroni, *An implicit/explicit spectral method for Burgers' equation*, Calcolo, 23, 1986, 265-284.

[7] N. Bressan and A. Quarteroni, *Analysis of Chebyshev collocation methods for parabolic equations*, Siam Journal on Numerical Analysis, 23, 1986, 1138-1154.

[8] J. Bruder, *Linearly-implicit Runge-Kutta methods based on implicit Runge-Kutta methods*, Applied Numerical Mathematics, 13, 1993, 33-40.

[9] M. P. Calvo, J. D. Frutos and J. Novo, *Linearly implicit Runge-Kutta methods for advection-reaction-diffusion equations*, Applied Numerical Mathematics, 37, 2001, 535-549.

[10] C. Canuto, *Boundary conditions in Chebyshev and Legendre methods*, SIAM Journal on Numerical Analysis, 23, 1986.

[11] C. Canuto, M. Y. Hussaini, A. Quarteroni and T. A. Zang, *Spectral Methods in Fluid Dynamics*, Springer-Verlag Berlin Heidelberg, 1988.

[12] T. F. Chan, *Stability analysis of finite difference schemes for the advection-diffusion equation*, SIAM Journal on Numerical Analysis, 21, 1984, 272-284.

[13] K. L. Cheng, W. Q. Feng, C. Wang and S. M. Wise, *An energy stable fourth order finite difference scheme for the Cahn-Hilliard equation*, Journal of Computational and Applied Mathematics, 362, 2019, 574-595.

[14] K. L. Cheng, Z. H. Qiao and C. Wang, *A third order exponential time differencing numerical scheme for no-slope-selection epitaxial thin film model with energy stability*, Journal of Scientific Computing, 81, 2019, 154-185.

[15] T. Colin and J.-M. Ghidaglia, *An initial-boundary value problem for the Korteweg-de Vries equation posed on a finite interval*, Advances in Differential Equations, 6, 2001, 1463-1492.

[16] J. Douglas Jr and T. Dupont, *Alternating-direction Galerkin methods on rectangles*, Numerical Solution of Partial Differential Equations-II, New York: Academic Press, 1971, 133-214.

[17] L. Duchemin and J. Eggers, *The explicit-implicit-null method: Removing the numerical instability of PDEs*, Journal of Computational Physics, 263, 2014, 37-52.

[18] J. Eggers, J. R. Lister and H. A. Stone, *Coalescence of liquid drops*, Journal of Fluid Mechanics, 401, 1999, 293-310.

[19] A. V. Faminskii, *Initial-boundary value problems in a rectangle for two-dimensional Zakharov-Kuznetsov equation*, Journal of Mathematical Analysis and Applications, 463, 2018, 760-793.

[20] M. Feistauer, J. Felcamn, M. Lukáčová-Medvid'ová and G. Warnecke, *Error estimates for a combined finite volume-finite element method for nonlinear convection-diffusion problems*, SIAM Journal on Numerical Analysis, 36, 1999, 1528-1548.

[21] F. Filbet and S. Jin, *A class of asymptotic-preserving schemes for kinetic equations and related problems with stiff sources*, Journal of Computational Physics, 229, 2010, 7625-7648.

[22] S. Gottlieb and C. Wang, *Stability and convergence analysis of fully discrete Fourier collocation spectral method for 3-D viscous Burgers equation*, Journal of Scientific Computing, 53, 2012, 102-128.

[23] E. Hairer and G. Wanner, *Solving Ordinary Differential Equations II*, Springer-Verlag Berlin Heidelberg, 1996.

[24] Y. H. Hao, Q. M. Huang and C. Wang, *A third order BDF energy stable linear scheme for the no-slope-selection thin film model*, Communications in Computational Physics, 29, 2021, 905-929.

[25] H. O. Kreiss and J. Oliger, *Comparison of accurate methods for the integration of hyperbolic equations*, Tellus, 24, 1972, 199-215.

[26] D. J. Korteweg and G. De Vries, *On the change of form of long waves advancing in a rectangular canal, and on a new type of long stationary waves*, Philosophical Magazine, 91, 2011, 1007-1028.

[27] D. Li and Z. H. Qiao, *On second order semi-implicit Fourier spectral methods for 2D Cahn-Hilliard equations*, Journal of Scientific Computing, 70, 2017, 301-341.

[28] D. Li, Z. H. Qiao and T. Tang, *Characterizing the stabilization size for semi-implicit Fourier-spectral method to phase field equations*, SIAM Journal on Numerical Analysis, 54, 2016, 1653-1681.

[29] W. J. Li, W. B. Chen, C. Wang, Y. Yan and R. J. He *A second order energy stable linear scheme for a thin film model without slope selection*, Journal of Scientific Computing, 76, 2018, 1905-1937.

[30] J. J. H. Miller, *On the location of zeros of certain classes of polynomials with applications to numerical analysis*, IMA Journal of Applied Mathematics, 8, 1971, 397-406.

[31] A. Mofid and R. Peyret, *Stability of the Chebyshev collocation approximation to the advection-diffusion equation*, Computers and Fluids, 22, 1993, 453-465.

[32] D. Pathria, *The correct formulation of intermediate boundary conditions for Runge-Kutta time integration of initial boundary value problems*, Siam Journal on Scientific Computing, 18, 1997, 1255-1266.

[33] D. Pavoni, *Single and multidomain Chebyshev collocation methods for the Korteweg-de Vries equation*, Calcolo, 25, 1988, 311-346.

[34] J. M. Sanz-Serna, J. G. Verwer and W. H. Hundsdorfer, *Convergence and order reduction of Runge-Kutta schemes applied to evolutionary problems in partial differential equations*, Numerische Mathematik, 50, 1987, 405-418.

[35] J. Schur, *Über Potenzreihen die im innern des Einheitskreises beschränkt sind*, Journal für die reine und angewandte Mathematik (Crelle's Journal), 147, 1916, 205-232.

[36] H. Shi and Y. Li, *Local discontinuous Galerkin methods with implicit-explicit multistep time-marching for solving the nonlinear Cahn-Hilliard equation*, Journal of Computational Physics, 394, 2019, 719-731.

[37] P. Smereka, *Semi-Implicit level set methods for curvature and surface diffusion motion*, Journal of Scientific Computing, 19, 2003, 439-456.

[38] M. Q. Tan, J. Cheng and C.-W. Shu, *Stability of high order finite difference and local discontinuous Galerkin schemes with explicit-implicit-null time-marching for high order dissipative and dispersive equations*, Journal of Computational Physics, 464, 2022, 111314.

[39] H. J. Wang, C.-W. Shu and Q. Zhang, *Stability analysis and error estimates of local discontinuous Galerkin methods with implicit-explicit time-marching for nonlinear*

convection-diffusion problems, Applied Mathematics and Computation, 272, 2016, 237-258.

[40] H. J. Wang, Q. Zhang, S. P. Wang and C.-W. Shu, *Local discontinuous Galerkin methods with explicit-implicit-null time discretizations for solving nonlinear diffusion problems*, Science China Mathematics, 63, 2020, 183-204.

[41] H. J. Wang, Q. Zhang and C.-W. Shu, *Third order implicit-explicit Runge-Kutta local discontinuous Galerkin methods with suitable boundary treatment for convection-diffusion problems with Dirichlet boundary conditions*, Journal of Computational and Applied Mathematics, 342, 2018, 164-179.

[42] C. J. Xu and T. Tang, *Stability analysis of large time-stepping methods for epitaxial growth models*, SIAM Journal on Numerical Analysis, 44, 2006, 1759-1779.

[43] J. Z. Zhu, L.-Q. Chen, J. Shen and V. Tikare, *Coarsening kinetics from a variable-mobility Cahn-Hilliard equation: Application of a semi-implicit Fourier spectral method*, Physical Review E, 60, 1999, 3564-3572.

Appendix A

Strategy of boundary treatment

For simplicity, we consider the linear convection-diffusion equation

$$U_t = \underbrace{dU_{xx} - a_1 U_{xx} - cU_x}_{T_1} + \underbrace{a_1 U_{xx}}_{T_2}$$

with boundary condition

$$U|_{\partial\Omega} = g(t).$$

where $c \in \mathbb{R}$ and $d > 0$ are the convection and diffusion coefficients, respectively, and a_1 is the stabilization parameter. We define two operators $\mathscr{A}$ and $\mathscr{B}$ such that

$$\mathscr{A}u^n = du^n_{xx} - a_1 u^n_{xx} - cu^n_x,$$

$$\mathscr{B}u^n = a_1 u^n_{xx}.$$

Then the third order IMEX Runge-Kutta scheme (2.8) implemented in interior reads

$$u^{n,1} = u^n, \tag{A.1a}$$

$$u^{n,2} = u^n + \tau\frac{1}{2}\mathscr{A}u^{n,1} + \tau\frac{1}{2}\mathscr{B}u^{n,2}, \tag{A.1b}$$

$$u^{n,3} = u^n + \tau\mathscr{A}\Big(\frac{11}{18}u^{n,1} + \frac{1}{18}u^{n,2}\Big) + \tau\mathscr{B}\Big(\frac{1}{6}u^{n,2} + \frac{1}{2}u^{n,3}\Big), \tag{A.1c}$$

$$u^{n,4} = u^n + \tau\mathscr{A}\Big(-\frac{1}{2}u^{n,1} + \frac{1}{2}u^{n,2} + \frac{1}{2}u^{n,3}\Big) + \tau\mathscr{B}\Big(\frac{5}{6}u^{n,2} - \frac{5}{6}u^{n,3} + \frac{1}{2}u^{n,4}\Big), \tag{A.1d}$$

$$\begin{aligned} u^{n,5} = {} & u^n + \tau\mathscr{A}\Big(-\frac{1}{4}u^{n,1} + \frac{7}{4}u^{n,2} + \frac{3}{4}u^{n,3} - \frac{7}{4}u^{n,4}\Big) + \\ & \tau\mathscr{B}\Big(\frac{3}{2}u^{n,2} - \frac{3}{2}u^{n,3} + \frac{1}{2}u^{n,4} + \frac{1}{2}u^{n,5}\Big). \end{aligned} \tag{A.1e}$$

We take the second stage as an example to show the idea. Note that

$$u^{n,2}_t = \mathscr{A}u^{n,2} + \mathscr{B}u^{n,2},$$

so from (A.1b) we have

$$\begin{aligned} u^{n,2} = {} & u^n + \tau\frac{1}{2}\mathscr{A}u^{n,2} + \tau\frac{1}{2}\mathscr{B}u^{n,2} + \tau\frac{1}{2}\mathscr{A}\big(u^{n,1} - u^{n,2}\big) \\ = {} & u^n + \tau\frac{1}{2}u^{n,2}_t + \tau\frac{1}{2}\mathscr{A}\big(u^{n,1} - u^{n,2}\big). \end{aligned}$$

Applying the operator $\mathscr{A}$ on both sides of (A.1b) we get

$$\begin{aligned}\mathscr{A}u^{n,2} =&\mathscr{A}u^n + \tau\frac{1}{2}\mathscr{A}^2u^{n,1} + \tau\frac{1}{2}\mathscr{A}\mathscr{B}u^{n,2}\\ =&\mathscr{A}u^n + \tau\frac{1}{2}\mathscr{A}^2u^{n,1} + \tau\frac{1}{2}\mathscr{A}\mathscr{B}u^{n,1} + O(\tau^2).\end{aligned}$$

Therefore,

$$u^{n,2} = u^n + \tau\frac{1}{2}u_t^{n,2} - \tau^2\frac{1}{4}\big(\mathscr{A}^2u^{n,1} + \mathscr{A}\mathscr{B}u^{n,1}\big) + O(\tau^3). \tag{A.2a}$$

Similarly,

$$u^{n,3} =u^n + \tau\frac{1}{6}\big(u_t^{n,2} + 3u_t^{n,3}\big) - \tau^2\frac{7}{18}\big(\mathscr{A}^2u^{n,1} + \mathscr{A}\mathscr{B}u^{n,1}\big) + O(\tau^3), \tag{A.2b}$$

$$u^{n,4} =u^n + \tau\frac{1}{2}\big(-u_t^{n,2} + u_t^{n,3} + u_t^{n,4}\big) - \tau^2\frac{5}{12}\big(\mathscr{A}^2u^{n,1} + \mathscr{A}\mathscr{B}u^{n,1}\big) + O(\tau^3), \tag{A.2c}$$

$$u^{n,5} =u^n + \tau\frac{1}{2}\big(3u_t^{n,2} - 3u_t^{n,3} + u_t^{n,4} + u_t^{n,5}\big) + O(\tau^3). \tag{A.2d}$$

From (A.1), we get $u_t^{n,s} = u_t(t_s^n)+O(\tau^2)$, $s = 2, ..., 5$ by Taylor expansion, where $t_s^n = t^n+\tilde{c}_s\tau$ is defined by (2.9). Replacing $u_t^{n,s}$ with $u_t(t_s^n)$ and extending the above scheme (A.2) up to boundary, we get the strategy of boundary treatment at intermediate stages

$$\tilde{g}^{n,2} =g^n + \tau\frac{1}{2}g_t(t^{n,2}) - \tau^2\frac{1}{4}\big(\mathscr{A}^2u^{n,1} + \mathscr{A}\mathscr{B}u^{n,1}\big)|_{\partial\Omega}, \tag{A.3a}$$

$$\tilde{g}^{n,3} =g^n + \tau\frac{1}{6}\big[g_t(t^{n,2}) + 3g_t(t^{n,3})\big] - \tau^2\frac{7}{18}\big(\mathscr{A}^2u^{n,1} + \mathscr{A}\mathscr{B}u^{n,1}\big)|_{\partial\Omega}, \tag{A.3b}$$

$$\tilde{g}^{n,4} =g^n + \tau\frac{1}{2}\big[-g_t(t^{n,2}) + g_t(t^{n,3}) + g_t(t^{n,4})\big] - \tau^2\frac{5}{12}\big(\mathscr{A}^2u^{n,1} + \mathscr{A}\mathscr{B}u^{n,1}\big)|_{\partial\Omega}, \tag{A.3c}$$

$$\tilde{g}^{n,5} =g^n + \tau\frac{1}{2}\big[3g_t(t^{n,2}) - 3g_t(t^{n,3}) + g_t(t^{n,4}) + g_t(t^{n,5})\big]. \tag{A.3d}$$

Obviously,

$$\tilde{g}^{n,s} = g^{n,s} + O(\tau^3),$$

where $g^{n,s}$ is the corresponding reference boundary condition. It is easy to obtain that

$$\mathscr{A}^2u^n = (d-a_1)^2u^n_{xxxx} + 2(a_1c-dc)u^n_{xxx} + c^2u^n_{xx},$$

$$\mathscr{A}\mathscr{B}u^n = a_1(d-a_1)u^n_{xxxx} - ca_1u^n_{xxx}.$$

The generalization of the strategy to the nonlinear and two-dimensional convection-diffusion and convection-dispersion equations is straightforward.